LAPPEENRANTA UNIVERSITY OF TECHNOLOGY
Faculty of Technology
Master's Degree Programme in Technomathematics and Technical Physics
Technical Physics

Sklyarova Anastasia

MÖSSBAUER SPECTRA OF IRON OXIDES IN THE BULK AND NANOCRYSTALLINE STATES

Examiners: Professor Erkki Lähderanta
Docent Johan Lindén

ABSTRACT

LAPPEENRANTA UNIVERSITY OF TECHNOLOGY
Faculty of Technology
Master's Degree Programme in Technomathematics and Technical Physics

Anastasia Sklyarova

MÖSSBAUER SPECTRA OF IRON OXIDES IN THE BULK AND NANOCRYSTALLINE STATES

Master's Thesis
2010
71 pages, 48 figures, 15 tables and 2 appendices
Examiners: Professor Erkki Lähderanta
Docent Johan Lindén

Keywords: nanoparticles, iron oxide, Mössbauer spectroscopy, magnetic properties

Magnetic nanoparticles are very important in modern industry. These particles are used in many different spheres of life.
Nanoparticles have unusual physical and chemical properties connected both with quantum dimensional effects and with the increased role of the surface atoms. Most clearly the difference between the properties of bulk materials and nanoparticles can be seen in the magnetic properties of these materials. The most typical magnetic properties of nanomaterials are superparamagnetism with the size of the cluster from 1 to 10 nm; single-domain magnetic state of nanoclusters and nanostructures up to 20 nm; magnetization processes connected with magnetic cluster ordering and with its forms and sizes; quantum magnetic tunneling effects when magnetization changes by jumps and giant magnetoresistance effects.
For research of the magnetic properties of iron-containing nanostructures, it is convenient to apply Mössbauer spectroscopy.
In this work a number of nano-sized samples of iron oxides were examined by Mössbauer spectroscopy. The Mössbauer spectra of nanoparticles with various sizes were obtained. Mössbauer spectra of iron oxide nanoparticles were compared with the spectra of bulk samples. It was shown how the spectra of iron oxide nanoparticles change depending on the particle sizes.

Contents

Introduction 3

Chapter 1. Theory of Mössbauer spectroscopy 5

1.1. The Mössbauer effect 5

1.2. Parameters of the Mössbauer spectra 6

1.3. Relative line intensities 9

Chapter 2. Literary overview 11

2.1. Bulk iron oxides 11

2.1.1. Bulk metallic iron (α-Fe) 11

2.1.2. Wustite (FeO) 12

2.1.3. Trivalent iron oxides (Fe_2O_3) 14

2.1.3.1. Hematite (α-Fe_2O_3) 14

2.1.3.2. Maghemite (γ-Fe_2O_3) 16

2.1.4. Magnetite (Fe_3O_4) 18

Summary of chapter 2.1 22

2.2. Iron nano-oxides 23

Overview 23

2.2.1. Iron oxide core-shell nanoparticles 23

Summary of chapter 2.2.1 39

2.2.2. Iron oxide nanoparticles 40

Summary of chapter 2.2.2 50

2.2.3. Clusters of iron oxide in matrices 51

Summary of chapter 2.2.3 55

Chapter 3. Experiment and discussion 56

3.1. Available samples 56

3.2. Studies 56

Conclusions 65

References 66

Appendix 1 68

Appendix 2 69

Introduction

Nanoparticles can be defined as particles that have at least one dimension less than 100 nanometers.

In recent years the study of nanostructures has been rapidly growing. A push in this direction was the occurrence and development of new methods of reception and research of nanostructures, the appearance of new nanomaterials and nanodevices. Progress in observation and research of nanostructures was made possible with the development of Tunneling and Scanning Microscopy, Radio-Frequency Microscopy, Mössbauer Spectroscopy and many other research methods.

Why have nanostructures attracted such intense interest? There are many reasons for the high interest to study nanostructures. These objects possess unusual physical and chemical properties connected both with quantum dimensional effects and with the increased role of surface atoms.

The most typical properties of nanomaterials are superparamagnetism with in clusters from ranging 1 to 10 nm; single-domain magnetic state of nanoclusters and nanostructures when dimensions reach 20 nm; magnetization processes which are connected with magnetic cluster ordering and with its forms and sizes; quantum magnetic tunneling effects when magnetization changes by jumps and giant magnetoresistance effects [1]. Also, as an example, it is possible to distinguish between Curie and Néel temperatures for bulk materials and nanostructures. Distinction between the properties of bulk materials and nanoparticles is clearly visible in the magnetic properties of these materials.

Many factors influence the magnetic properties of nanoparticles, e. g.: chemical formula (structure), type of crystal lattice and level of lattice imperfection, size and shape of particles, interaction between cluster and matrix as well as between clusters themselves.

It is possible, in certain limits, to control the magnetic characteristics of a material by changing sizes, form, compound and structure of nanoparticles. However, the properties of same nanomaterials can strongly differ because the monitoring process of all factors affecting the properties of synthesised nanoobjects is rather complicated.

In order to study the magnetic properties of iron-containing nanostructures, it is convenient to use Mössbauer spectroscopy. This research method offers the possibility to investigate bulk crystalline materials, amorphous ones, and – what is important for us – materials with nanoscaled crystallite sizes. This method gives information on static properties of investigated materials (phase structure, magnetic state, crystal lattice, valence state) and about dynamic properties (superparamagnetic relaxation, diffusion, etc.). Mössbauer spectroscopy gives also information about interactions inside the clusters, about intercluster interactions and interactions between nanoparticles and the surrounding matrix. Owing to the high resolution and high sensitivity, this method enables selective studies on properties both inside and on the surface of the nanoparticles.

The purpose of this work is to compare the Mössbauer spectra of nanocrystalline iron oxides and bulk iron oxides for clearer identification studied nano-sized samples.

Chapter 1. Theory of Mössbauer spectroscopy

1.1. The Mössbauer effect [2,3]

Mössbauer spectroscopy is a spectroscopic technique based on the recoil-free, resonant absorption and emission of gamma rays in solids. The phenomenon of nuclear gamma resonance was first observed by Rudolf Mössbauer in 1957.

Emission or absorption of gamma quanta by free atomic nuclei is accompanied by change of radiation energy due to loss of recoil energy:

$$E_R = \frac{E_\gamma^2}{2mc^2}, \quad (1)$$

where E_γ is the energy of gamma rays, m is the mass of the nucleus, and c is the speed of light. As a result of this nuclear recoil the energy of the emitted gamma ray is less than the energy difference between the two nuclear levels. If resonant absorption is to occur the energy of the incoming gamma rays needs to be greater than this energy difference. Thus for free nuclei the recoil energy prevents resonant absorption of gamma rays under normal circumstances. However, when the emitting and absorbing nuclei are bound in a solid, a certain fraction of gamma rays are emitted and absorbed with negligible energy loss due absence of recoil. The energy is transferred to the whole lattice, which is massive and therefore the energy loss is even smaller than given by the uncertainly relation.

For observation of the Mössbauer effect a long-living nuclear levels are used with transition energies of no more than 200 keV and life times of 10^{-6} to 10^{-10} s. Most often the Mössbauer effect is observed on the ^{57}Fe nucleus. For this nucleus the energy is E_g = 14.4 keV, the life time is $1.4 \cdot 10^{-7}$ s, the probability of the Mössbauer effect is ~ 0.8 and the line width is $\Gamma = 4.7 \cdot 10^{-9}$ eV.

In order to observe a resonant absorption it is necessary to modulate the gamma ray energy using the Doppler effect. The change in energy is given by:

$$\Delta E_v = \frac{vE_\gamma}{c}. \quad (2)$$

In the resulting spectra, gamma rays intensity is plotted as a function of the source velocity (v).

1.2. Parameters of the Mössbauer spectra

Using Mössbauer spectroscopy one may probe the tiny changes in the energy levels of an atomic nucleus in response to its environment. Due to the high energy and extremely narrow line widths of the gamma rays, Mössbauer spectroscopy is one of the most sensitive techniques in terms of energy (and hence frequency) resolution, capable of detecting change in just a few parts per 10^{11}. Typically, three types of nuclear interaction may be observed: the isomer shift, also known as the chemical shift; the quadrupole splitting; and, magnetic or hyperfine splitting, also known as the Zeeman effect. The main parameters of Mössbauer spectra are:

1. **The probability of the Mössbauer effect** is connected with solid-state characteristics such as root mean square (rms) of atomic displacements in the lattice and the wave vector of a resonant gamma-quantum. Furthermore, the Mössbauer resonance line has doubled natural width as a result of the summation of the source and absorber widths. The source and the absorber consist of identical nuclei.

2. **The effective line width.** The natural line width is given by the uncertainty relation: $\Gamma = \hbar / \tau$, where $\hbar = h / (2\pi)$ and τ is the life time of the excited state of the Mössbauer nuclei. With small absorber thickness the spectral lines have Lorentzian shapes. The line width can be used for definition of the areas of spectral lines and, hence, the amount of resonant atoms in a specific chemical environment.

3. **The isomer shift (δ)** is a relative measure describing a shift in the resonance energy of a nucleus due to the interaction with electrons in the *s* orbital. The whole spectrum is shifted either in positive or negative direction depending upon the *s* electron charge density. This change arises due to changes in the electrostatic response between the non-zero probabilities for orbital electrons to occupy the non-zero volume of the

nucleus the electrons orbit.

Only *s* electrons exhibit non-zero probability because their spherical shape incorporates the volume taken up by the nucleus. However, the *p*, *d*, and other electrons may influence the *s* electron density through a screening effect. The *s* electron density can also be affected by the spin and oxidation state and the chemical environment of the atom.

The δ value is defined by the formula:

$$\delta = \frac{4\pi}{5} e^2 Z R^2 \frac{\Delta R}{R} \{|\psi(0)|_n^2 - |\psi(0)|_u^2\}, \quad (3)$$

where e is the electron charge, Z the nuclei charge number, ΔR the change of the nuclear radius due to the γ transition, $|\psi(0)|_n^2$ and $|\psi(0)|_u^2$ are electronic densities the resonant nuclei in the absorber and the source, respectively. Experimentally the isomer shift is defined as a shift of the whole spectrum with respect to a standard velocity.

The value of the isomer shift gives information about the valence state of the resonant atom in the investigated substance.

4. **Magnetic Splitting (hyperfine splitting)** is a result of the interaction between the nucleus and the surrounding magnetic field. A nucleus with spin, I, splits into $2I + 1$ sub-energy levels in the presence of a magnetic field. For example, a nucleus with spin state $I = 3/2$ will split into 4 non-degenerate sub-states with m_I values of +3/2, +1/2, -1/2 and -3/2. The energy of the each split is 10^{-7} eV. The quantum-mechanical selection rules of magnetic dipoles enable transitions between the excited state and the ground state where m_I changes by 0 or ± 1. This gives six possible transitions for a 3/2 to 1/2 transition.

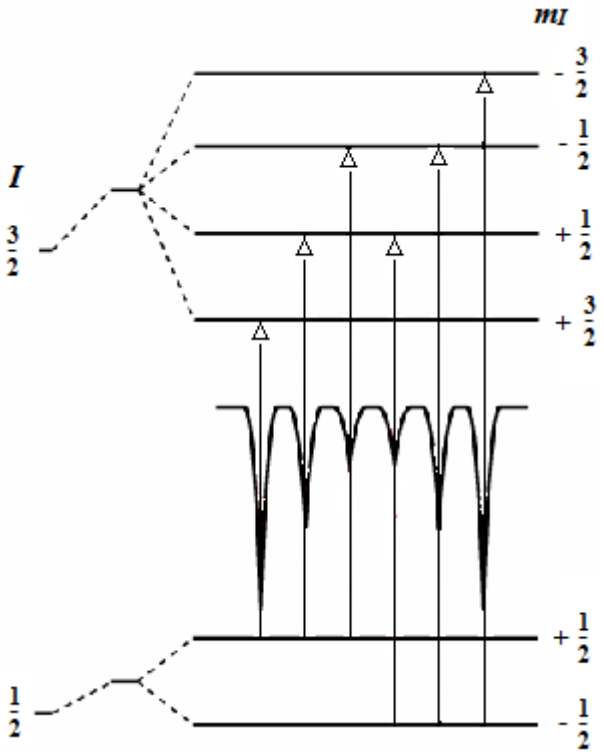

Fig.1 Magnetic splitting of the nuclear energy levels.

Therefore, in most cases, only six peaks can be monitored in a spectrum produced by identical hyperfine-split nuclei.

5. Electric quadrupole splitting

Quadrupole Splitting (QS) reflects the interaction of the nuclear energy levels with the surrounding electric field gradient (EFG). Nuclei in states with non-spherical charge distributions, i.e. all those with nuclear spin quantum numbers (I) greater than 1/2, produce non-zero quadrupole moments which split the nuclear energy levels if the nucleus is subjected to a non-zero EFG.

In the case of an isotope in a excited state with I = 3/2, such as ^{57}Fe or ^{119}Sn, the 3/2 to 1/2 transition splits into two substates m_I = ± 1/2 and m_I = ± 3/2. These appear as two specific peaks in a spectrum, sometimes referred to as a 'doublet'. Quadrupole splitting is measured as the distance between these two peaks and it reflects the character of the electric field

at the nucleus, which in turn depends mainly on the local ionic structure around the atom.

6. Temperature (Doppler) shift

Nuclear fluctuations in a solid can lead to a modulation of the energy of the resonant gamma quanta. But, because the life time of a Mössbauer level (10^{-5} - 10^{-10} s) is longer than the typical time of nuclear fluctuations (~ 10^{-15} s) the effect is averaged out. As a result the first-order Doppler effect is absent. However, the second-order Doppler effect exists because it is proportional to the square of the speed, which is not averaged out. Then, the temperature (Doppler) shift can be found as:

$$\delta_R = -\frac{V^2}{2c^2} \cdot E_\gamma. \tag{4}$$

This shift depends on temperature as:

$$\delta_R \sim -\frac{3k_B T}{2mc^2}. \tag{5}$$

Using the parameters of the experimental Mössbauer spectra, it is possible to obtain useful information on the structure and the properties of the investigated substances.

1.3 Relative line intensities [1, 2]

The line positions are connected to the splitting of the energy levels, but the line intensities are connected to the angle between the Mössbauer gamma-rays and the nuclear spin moment. The outer-, middle- and inner-line intensities in a six-line spectrum are related by:

$$3: (4\sin 2\theta)/ (1+\cos 2\theta): 1 \tag{6}$$

indicating that the outer and inner lines are always in the same proportion but the middle lines can vary in relative intensity between 0 and 4 depending on the angle θ that the nuclear spin moments make form with the gamma-rays. This leads to a relative line intensities, of 3: 0: 1: 1: 0: 3 for $\theta = 0^0$, and 3: 4: 1: 1: 4: 3 for $\theta = 90^0$, when magnetic hyperfine structure is present.

In polycrystalline samples with no applied field the values of the 2nd and the 5th lines average to 2 (as in Fig. 2) but in single crystals or under applied fields the relative line intensities can give information about the orientation of the magnetic moments and the magnetic ordering.

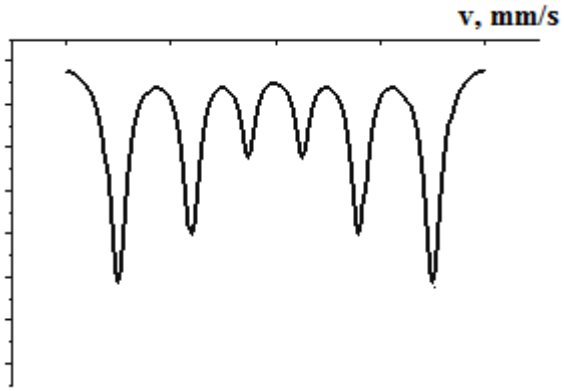

Fig. 2. Relative intensities of lines for polycrystalline materials.

For spectra exhibiting quadrupole splitting the line intensities are related to the angle θ_q between the Mössbauer gamma-rays and the electric field gradient.

The asymmetry parameter (η) specifies the deflection from the axial symmetry for the EFG. The asymmetry parameter is defined as:

$$\eta = \frac{|V_{xx} - V_{yy}|}{V_{zz}}, \tag{7}$$

where V_{xx}, V_{yy}, V_{zz} are the principal components of EFG tensor.

In the case of the axial symmetry ($\eta = 0$) angular dependences for the line intensities will be $(1 + \cos\theta_q)$ and $(2/3 + \sin\theta_q)$ for transitions with $\Delta m = \pm 1$ and $\Delta m = 0$, accordingly. This relation gives a line intensities ratio of 3 : 1 and 3 : 5

for $\theta_q = 0^0$ and $\theta_q = 90^0$, accordingly. For polycrystalline materials with random orientation the ratio of line intensities is 1 : 1.

Chapter 2. Literary overview

2.1. Bulk iron oxides

For interpretation of the Mössbauer spectra correlation of spectral parameters with various Fe-O phases is necessary. Over the years several papers have been written as the ^{57}Fe isotope is commonly used in Mössbauer studies.

In this overview information from various studies on bulk iron oxides is collected. Also the parameters obtained from the Mössbauer spectra are summarized.

2.1.1. Bulk metallic iron (α-Fe)

The Mössbauer spectrum for bulk metallic iron is well known. The Mössbauer spectrum of bulk metallic α-Fe is used as a common standard reference for the isomer shift of spectra. The Mössbauer spectrum obtained by the 14.4 keV transition of bulk ^{57}Fe in the metallic condition represents a simple example of a pure Zeeman effect. The quadrupole splitting of the nuclear energy levels is absent because the lattice of iron has cubic symmetry. At room temperature the spectrum shows a magnetic sextet. If magnetic domains, and, hence, internal fields have random orientation the line intensities of the magnetic sextet are related by 3:2:1:1:2:3. The magnitude of the internal magnetic field acting on the Fe nuclei was first measured in [4]. At 300 K its value was found to be 33.3 T.

Studies of the Mössbauer spectra of various iron compounds, have given the values of the isomer shifts for various valence conditions of iron (Table 1).

Table 1. Isomer shifts in mm/s for various valence conditions of Fe at room temperature [4].

Fe^{2+} $3d^6$	Fe^{3+} $3d^5$	Fe^{4+} $3d^4$	Fe^{6+} $3d^2$
(0.65) - (1.45)	(0.05) - (0.5)	(-1.15) - (0.05)	(-0.35) - (-0.45)

2.1.2. Wustite (FeO)

Literature data for iron oxide FeO show that wustite has cubic crystal structure and exhibits ferromagnetic properties. The Curie temperature of this oxide is equal to 198 K. Wustite has a non stoichiometric structure ranging from $Fe_{0.95}O$ to $Fe_{0.89}O$. The lack of cation is defined by preparation conditions of FeO. At room temperature wustite is paramagnetic. For wustite the magnetic parameters dependence on the stoichiometry are shown in Fig. 3.

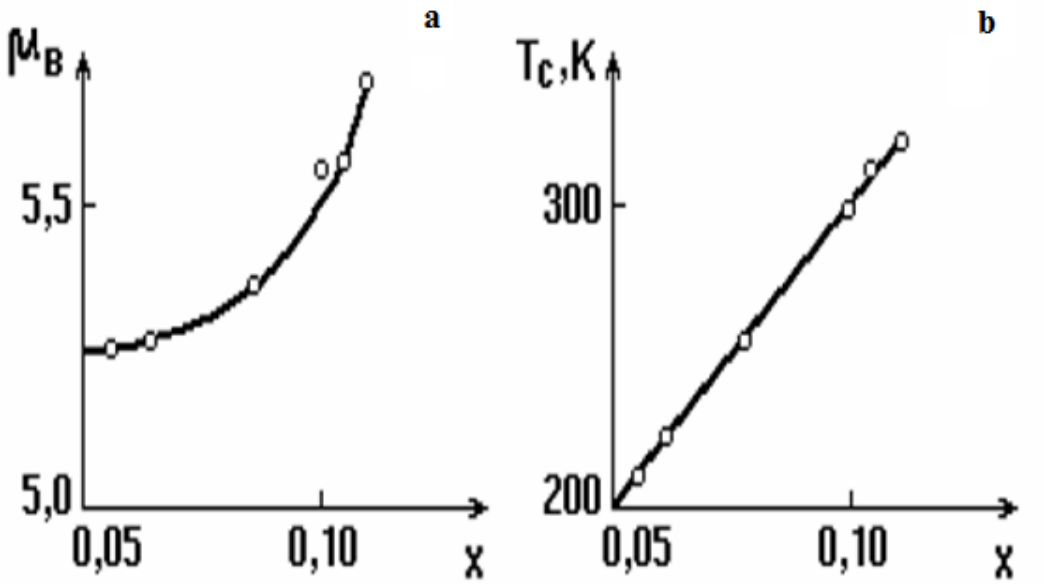

Fig. 3 The effective magnetic moment and the Curie temperature dependence on stoichiometry of structure $Fe_{1-x}O$.

At temperature 90 K wustite has a structural phase transition from face-centered cubic lattice to a rhombohedral lattice. In this transition, the magnetic properties of wustite change. The Mössbauer spectrum of wustite is a singlet at room temperature or a doublet with a very small quadrupole splitting. As in example, the Mössbauer spectrum of $Fe_{0.915}O$ is shown in Fig. 4.

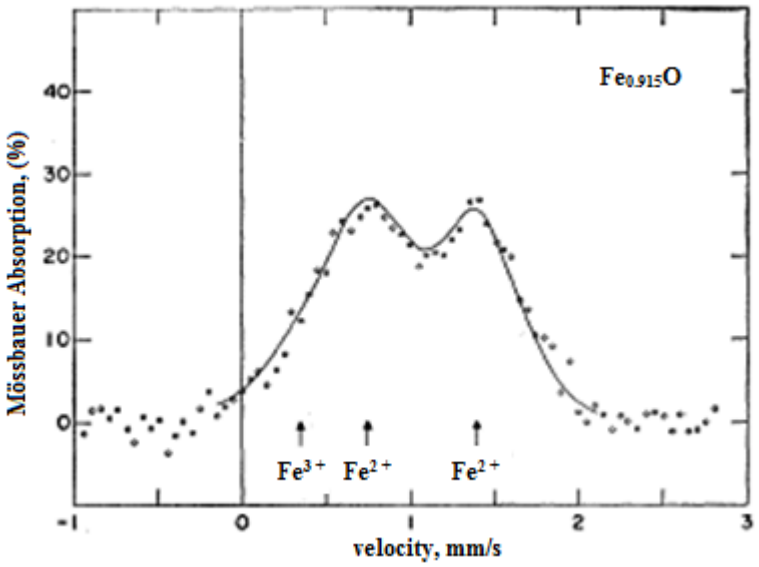

Fig. 4 The Mössbauer spectrum of oxide $Fe_{0.915}O$. The continuous line represents superposition 8 Fe^{2+} components dna 1 Fe^{3+} component in the ratio 4:4:1 [1].

The Mössbauer parameters for several FeO samples are given in Table 2 [5]. Two absorption lines were measured [5] in Fe^{2+} and Fe^{3+} in lattice.

Table 2. The Mössbauer parameters of several FeO samples.
The isomer shifts are measured relative to α-Fe.

Oxide	***IS*, mm/s**	***QS*, mm/s**
$Fe_{0.941}O$	1.42	0.30
$Fe_{0.919}O$	1.42	0.34
$Fe_{0.915}O$	1.42	0.32

2.1.3. Trivalent iron oxides (Fe_2O_3)

Trivalent iron oxides Fe_2O_3 exist in two forms: α-Fe_2O_3 and γ-Fe_2O_3.

2.1.3.1. Hematite (α-Fe_2O_3)

Oxide α-Fe_2O_3 has a corundum structure. The Fe^{3+} ions occupy 2/3 of the octahedral positions among the hexagonally close packed oxygen ions. Hematite is antiferromagnetic at temperatures below the Néel temperature (675 °C). In the temperature interval -20°C < T < 675°C hematite exhibits weak ferromagnetic properties that are the result of the canted arrangement of the magnetic moments of the sublattices. In this temperature interval the magnetic moments of ions Fe^{3+} are directed at right angles to the rhombohedral axis of the hematite structure. At temperatures below -20°C the magnetic moments turn along the rhombohedral axis. Such a transition is known as the Morin transition. At the Néel point (675°C) hematite passes from a weak ferromagnetic state into the paramagnetic state. The magnetic susceptibility of hematite is $\chi = 80 - 260 \cdot 10^{-9}$ m^3/kg, and the value of saturation specific magnetization is $J_s = 0.36 \cdot 10^{-7}$ T· m^3/kg.

A typical Mössbauer spectrum of α-Fe_2O_3 oxide consists of a typical sextet as shown in Fig. 5 [6]. The values of the Mössbauer parameters are presented in Table 3.

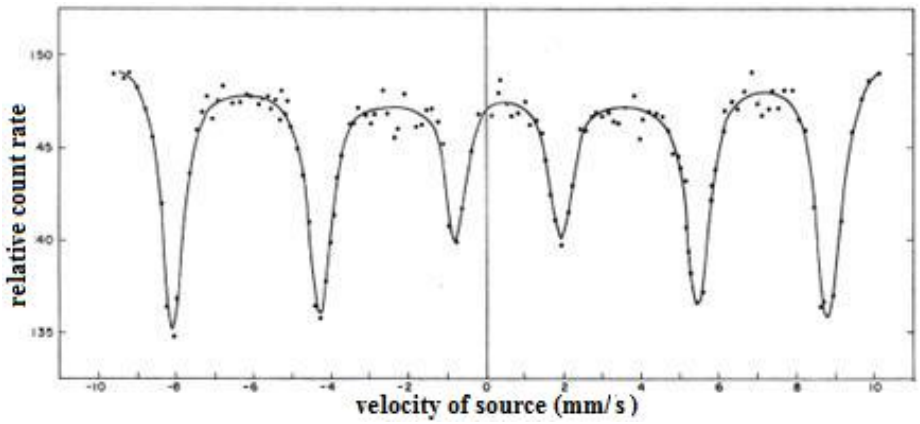

Fig. 5 The Mössbauer spectrum of hematite, T = 298K.

Table 3. Hyperfine parameters of α-Fe_2O_3 at 25°C. Isomer shift is measured relative to α-Fe.

***IS*, mm/s**	***QS*, mm/s**	***B*, T**
0. 56 ± 0.03	0.24 ± 0.03	51.5

In [7] another spectrum of hematite measured at temperature 300 K is presented, Fig.6. The parameters of the Mössbauer spectra of α-Fe_2O_3 at the various temperatures are presented in Table 4.

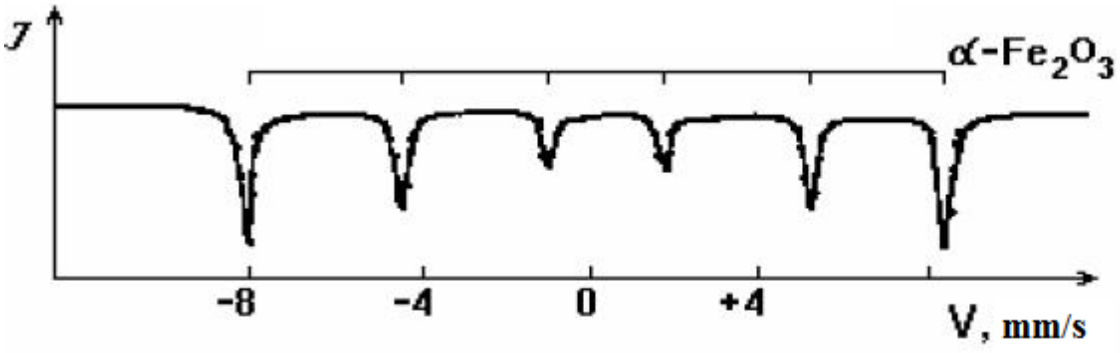

Fig. 6 The Mössbauer spectrum of hematite, T = 300 K.

Table 4. The Mössbauer parameters of α-Fe_2O_3; isomer shift is measured relative to sodium nitroprussid.

***T*, K**	***B*, T**	***IS*, mm/s**	***QS*, mm/s**
298	51.8	0.74	-0.21
78	54.2	-	0.34
4	54.5	-	-

Comparing the spectra and the Mössbauer parameters, it is possible to conclude that the Mössbauer spectra of bulk hematite are similar for various works. The values for the effective magnetic fields acting on the iron nuclei coincide for various works in literature. At the same time, a scattering of the quadrupole

splitting values and the isomer shifts for various measurements are observed. For the isomer shift it can be a consequence of a recalculation of the values because the isomer shift was presented against various standards in the measurements.

2.1.3.2. Maghemite (γ-Fe_2O_3)

Maghemite has a spinel structure in which a part of the cation positions are vacant. The environment of ion Fe^{3+} in the lattice can be either octahedral or tetrahedral. This iron oxide is thermally unstable. At temperatures above 220 – 300°C undergoes an irreversible transition into hematite (α-Fe_2O_3). The Curie temperature of maghemite is 675 °C. The magnetic susceptibility of maghemite is $\chi = 3 - 20 \cdot 10^{-4}$ m^3/kg, and the specific saturation magnetization is $J_s = 88 \cdot 10^{-7}$ T· m^3/kg (magnetization in a field of B = 2.5 T at T = 300 K).

Though at temperatures below the Curie temperature, the maghemite is ferrimagnetic; at room temperature the Mössbauer spectrum of maghemite consists of six lines. In [8] the spectrum of maghemite was obtained at 85 K (see Fig. 7). The corresponding Mössbauer parameters are calculated at 300 K and 85 K (see Table 5).

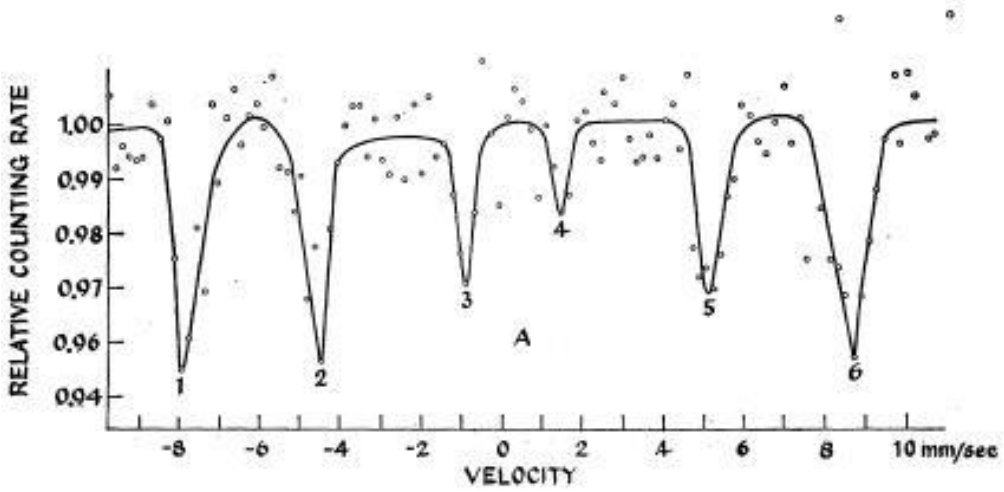

Fig. 7 The Mössbauer spectrum of γ-Fe_2O_3, T = 85 K.

Table 5. The Mössbauer parameters of γ - Fe_2O_3.

***T*, K**	***Γ*, mm/s**	***IS*, mm/s**	***QS*, mm/s**	***B*, T**
300	5.95 ± 0.20	0.5 ± 0.05	-0.1 ± 0.1	50.5 ± 2.0
85	6.05 ± 0.20	0.4 ± 0.1	0.1 ± 0.1	51.5 ± 2.0

In Fig. 8 the spectrum of this iron oxide is shown at room temperature [7].

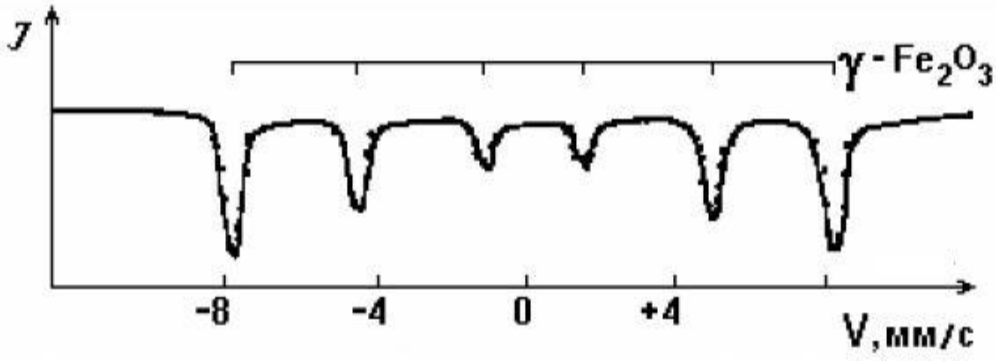

Fig. 8 The Mössbauer spectrum of γ - Fe_2O_3 at T = 298 K.

Table 6. The Mössbauer parameters of maghemite. Isomer shifts are measured relative to sodium nitroprussid.

***T*, K**	***B*, T**	***IS*, mm/s**	***QS*, mm/s**
298	49.9	0.37	0.02
78	52.7	0.46	-

Thus, a certain coincidence of the few spectra and the values of the effective magnetic field and the quadrupole splitting for various bulk samples of maghemite are observed. However, as well as for hematite, there is a scattering in isomer shift values.

2.1.4. Magnetite (Fe_3O_4)

Magnetite is ferromagnetic at temperature above 858 K and has an inverse spinel structure. The distribution of the cations is given by (Fe^{3+}) [$Fe^{2+}Fe^{3+}$] O_4. The magnetic properties of magnetite are defined by an indirect magnetic interaction of the iron ions which occupy the octahedral (A-positions) and the tetrahedral positions (B-positions) (see Fig. 9).

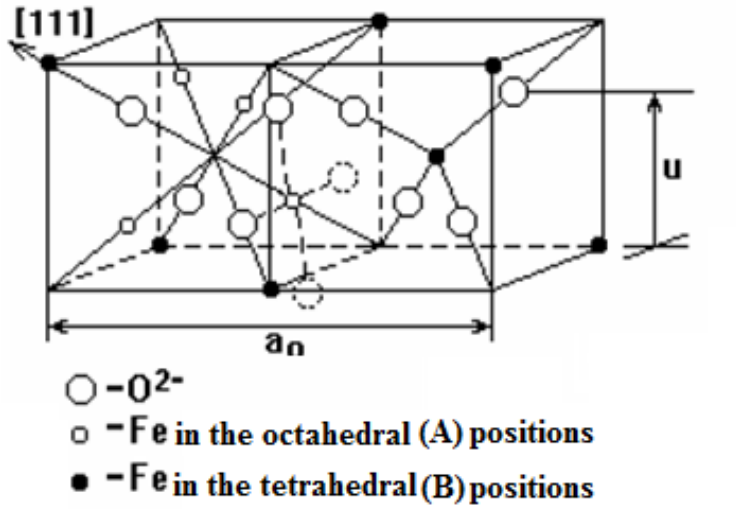

Fig. 9 The magnetite structure.

In stoichiometric magnetite there are twice as many octahedral positions than tetrahedral positions. The magnetic properties of magnetite are well studied. Its magnetic susceptibility is χ = 3 - $20 \cdot 10^{-4}$ m^3/kg, the specific saturation magnetization of magnetite is J_s = $97 \cdot 10^{-7}$ $T \cdot m^3/kg$ (magnetization in a field of B = 2.5 T at the temperature T = 300 K). At -150 °C magnetite undergoes the Verwey transition [9]. In the Fig. 10 can be seen that at -150 °C the magnetization of stoichiometric magnetite has a local maximum.

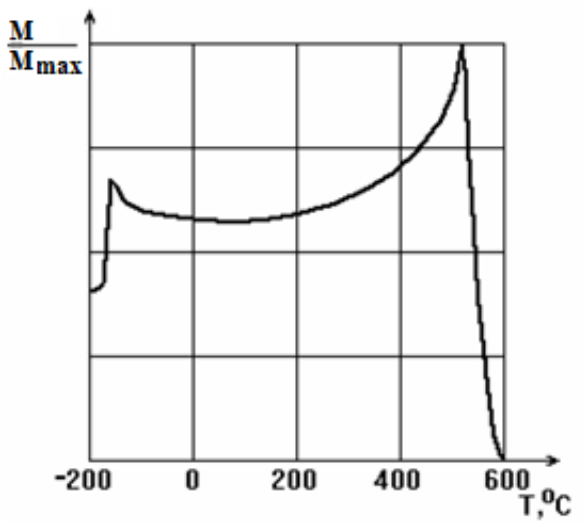

Fig. 10 Thermo-magnetic curve of magnetite.

E.Verwey assumed that at -150 °C there is a structural phase transition. The magnetic anisotropy constant passes through zero and changes the sign. This leads to occurrence of a magnetization maximum on the thermo-magnetic curve.

A ferromagnetic-to-paramagnetic transition at the Curie temperature is responsible for a second peak in the curve. In weak magnetic fields the so-called Gopkinson effect is observed. At approximately 500 °C a sharp increase of value of magnetization is observed before its falling. This effect is due to the approach to zero for the constants of magnetic crystallographic anisotropy and magnetostriction.

At temperatures above the Verwey point and close to room temperature the Mössbauer spectra of magnetite has two sextets. The line intensities of these sextets are related as 2 : 1 (octahedral positions: tetrahedral positions).

The spectrum of magnetite is very complicated. In 1961 a group of scientists [8] investigated hyperfine magnetic interactions in magnetite in the temperature range 85 – 300 K. The results are given in Fig. 11 and in Table 7.

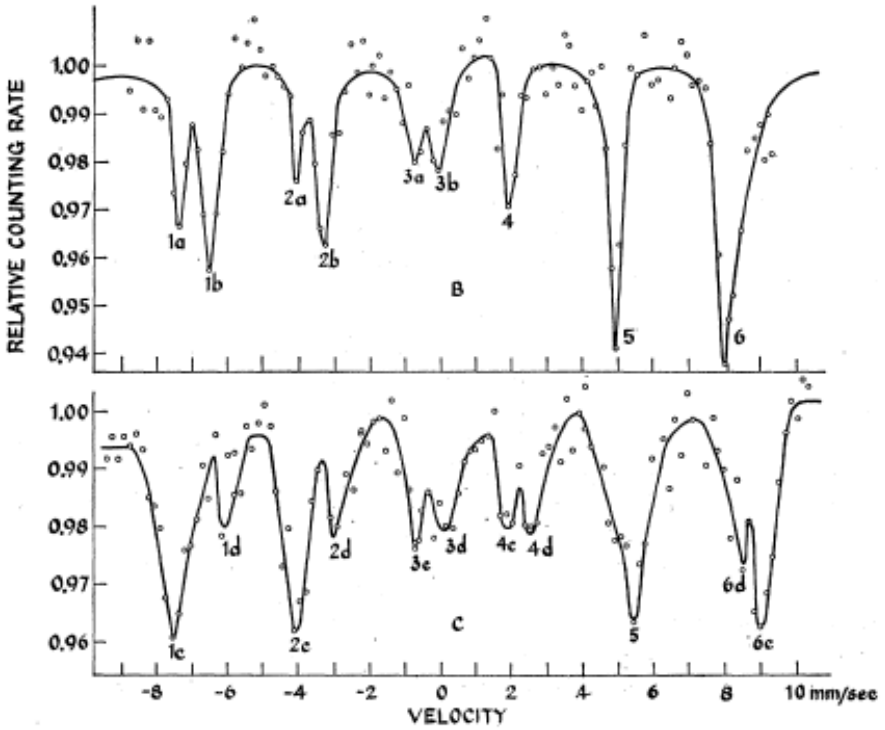

Fig. 11 The Mössbauer spectra of Fe_3O_4 at 300 K (the top spectrum) and at 85 K (the bottom spectrum).

Table 7. The Mössbauer parameters of magnetite at temperatures of 300 K and 85 K. Isomer shifts are measured relative to α-Fe.

***T*, K**	***Γ₀*, mm/s**	***Γ₁*, mm/s**	***IS*, mm/s**	***QS*, mm/s**	***B*, T**
85	0.605 ± 0.020	0.345 ± 0.015	0.74 ± 0.10	0.00 ± 0.10	51 ± 2
	0.54 ± 0.025	0.300 ± 0.015	1.24 ± 0.15	0.00 ± 0.10	45 ± 2
300	0.590 ± 0.020	0.335 ± 0.015	0.56 ± 0.10	0.0 ± 0.1	50 ± 2
	0.53 ± 0.02	0.31 ± 0.01	0.79 ± 0.1	0.0 ± 0.1	45 ± 2

In Fig. 12 is shown a typical spectrum of magnetite at room temperature [7]. Apparently from drawing, it is possible to identity two sextets of lines in the spectrum. The Mössbauer parameters of this spectrum are presented in Table 8.

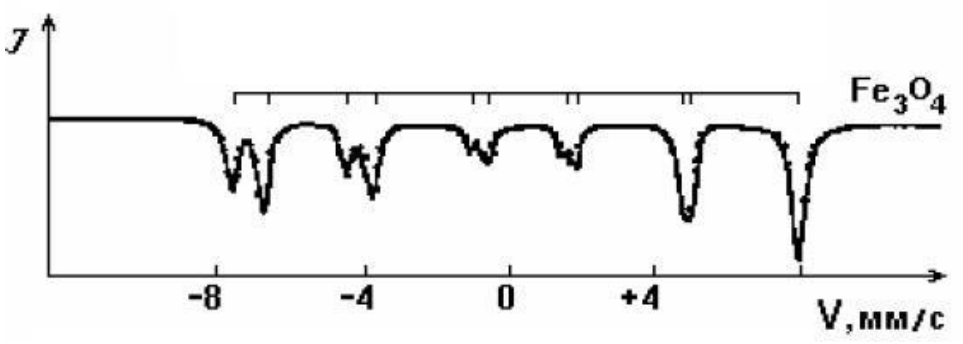

Fig. 12 The Mössbauer spectrum of Fe_3O_4 at 300 K.

Table 8. The Mössbauer parameters of magnetite. Isomer shifts are measured relative to α-Fe.

***T*, K**	***B*, T**	***IS*, mm/s**	***QS*, mm/s**
300	50.7	0.32	0.005
	45.0	0.35	0.003

At 77 K the value of the effective magnetic field acting on the iron nuclei increases to 51.5 T.

Thus, it is possible to notice that for stoichiometric magnetite is observed an invariable kind of the spectrum at room temperature. Scattering of the effective fields values on iron nuclei is also observed for the reported works.

Summary of chapter 2.1

Thus, having compared the data from references on volume samples, it is possible to conclude:

1. The shape of the Mössbauer spectra of bulk iron oxides coincide for the reported works.
2. The average values of the effective magnetic fields acting on the nuclei are 50.0 T (for maghemite) and 51.6 T (for hematite). For magnetite small disorder in sizes of the effective fields acting on the nuclei of iron was observed (disorder of values makes 5 %).
3. Disorder of quadrupole splitting and isomer shift values for various measurements is observed. For the isomer shift it can be a consequence of the choice of isomer shift standard used in the various measurements.

2.2. Iron nano-oxides

Overview

In the previous chapter of this work, properties of bulk iron oxides were considered. However, at nanoscale dimentions the properties of the studied objects can differ from the properties of bulk materials. Also, the correlation between the Mössbauer parameters and the condition of materials can change.

In this chapter, Mössbauer spectroscopy of nanoscale samples of iron oxides is considered. In this part of review, the literature results received for the nano-oxides are compared with the results for the bulk oxides (see also the previous chapter).

2.2.1. Iron oxide core-shell nanoparticles

In the course of iron combustion, a film consisting of nanooxide particles having the nanosize is formed on surface of iron. In 1987 Maeda, et al. [10] studied in the temperature range 4.2 – 298 K of iron particles with different oxidation times and formation of the oxidized films on the surface of thin iron particles. Experimental samples contained metallic α-Fe and an iron oxide with the spinel structure. The particles of the investigated samples had a needle-type shape with diameters of about 15 nm and lengths of 100 nm. The spectra of the samples at 298 K are presented in Fig. 13.

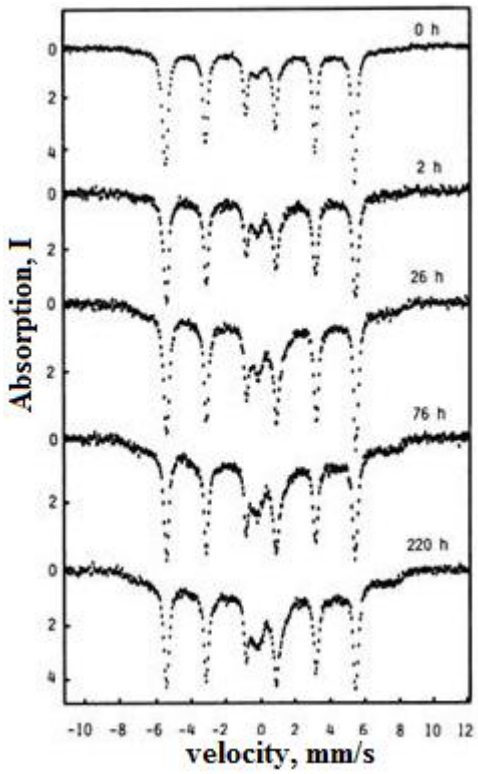

Fig. 13 The Mössbauer spectra of iron oxide nanoparticles at different times of oxidation, T = 298 K [10].

In the figure, the spectrum of the initial powder of iron consists of a magnetic sextet arising from metallic iron, and a paramagnetic doublet. The doublet has been attributed by the authors to the iron oxide [10]. In the course of combustion of iron, the width of the spectral lines increases. For metallic iron, the sextet has narrow lines and the size of the hyperfine field (B_{HF}) coincides with that of standard α-Fe. At 78 K the spectrum is a superposition of the sextets (see Fig. 14) doe to magnetic hyperfine structure for iron and for the iron oxide. At the lower temperature the doublet due to the oxide condition transforms into the magnetic sextet. Such a transformation indicates the transition of an oxide into the magnetically ordered state.

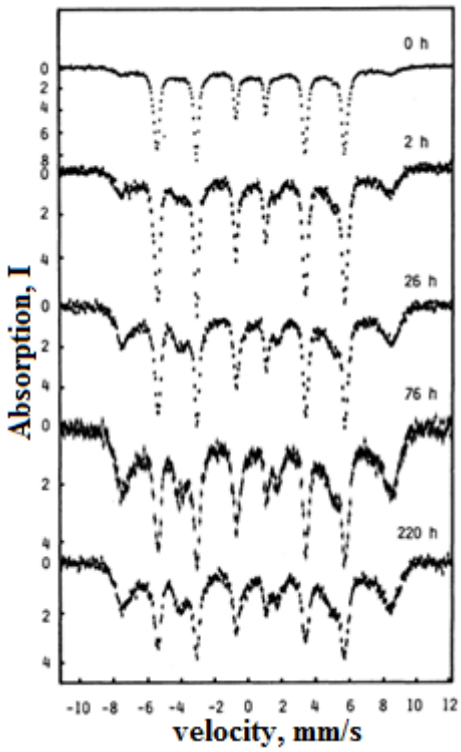

Fig. 14 The Mössbauer spectra of samples at 78 K [10].

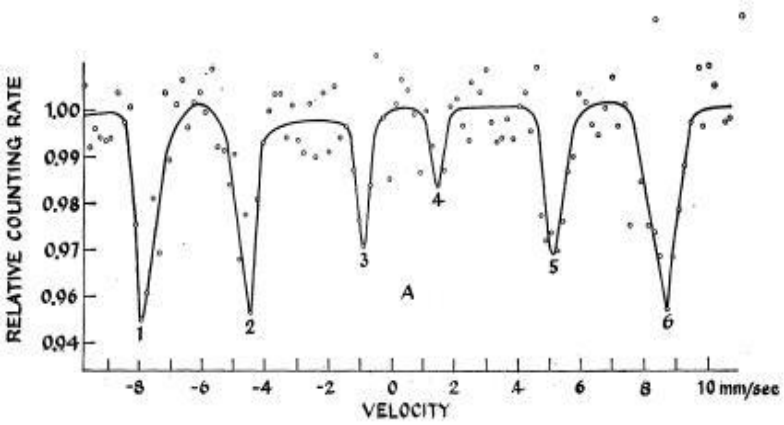

Fig. 15 The Mössbauer spectrum of bulk maghemite at 85 K [8].

Values of the Mössbauer parameters are presented in Table 9.

Table 9. The Mössbauer parameters of the samples measured at 78 K. *F* is the ratio between the area of iron oxide and the total area of particle, *d* is the diameter of the metallic iron core.

	Metallic iron			**Iron oxide**						
Annealing time of the samples (hours)	***IS*, mm/s**	***B*, T**	***Γ*$_1$, mm/s**	***IS*, mm/s**	***QS*, mm/s**	***B*, T**	***Γ*$_1$, mm/s**	***Γ*$_6$, mm/s**	***F*, %**	***d*, nm**
0	0.168	34.5	0.405	0.549	-0.275	49.2	0.657	0.919	29	12.2
2	0.170	34.5	0.388	0.585	-0.336	48.7	1.398	1.222	44	10.6
8	0.163	34.5	0.440	0.575	-0.245	49.0	1.199	1.331	51	9.8
26	0.163	34.5	0.412	0.562	-0.280	48.9	1.208	1.250	57	9.2
76	0.171	34.6	0.469	0.487	-0.009	48.8	1.231	1.315	63	8.4
220	0.170	34.6	0.542	0.463	+0.079	48.8	1.315	1.389	61	8.8

Studying the Mössbauer spectra in different temperatures, the authors have found that the oxide sextet is due to γ-Fe_2O_3. It was identified from the absence of the Verwey transition. At 4.2 K the spectrum contains two sextets (see Fig. 16) which clear show presence of iron and iron oxide in the sample. The values of the Mössbauer parameters for the oxidized part of the spectrum are B = 49.8 T, IS = 0.451 mm/s and QS = 0.00 mm/s.

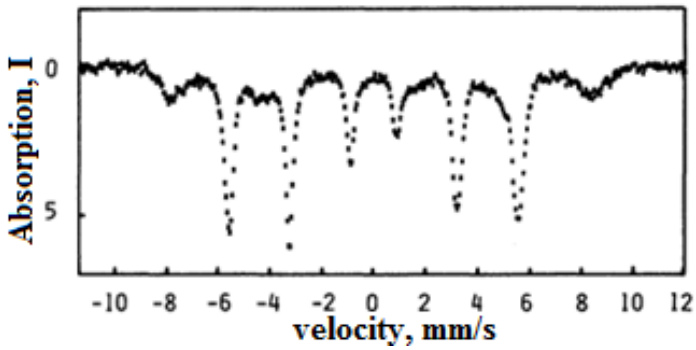

Fig. 16 The Mössbauer spectrum of primary powder of iron at 4.2 K [10].

Comparing the data for bulk maghemite and the results in [10] shows that for nanoscale maghemite the hyperfine field decreases in comparison with the bulk samples (for the bulk samples: 51.5 – 52.0 T at 78 K and 52.7 T at 4.2 K; for nanoscale samples: 48.7 – 49.2 T at 78 K and 49.8 T at 4.2 K). With an oxidation time of 76 - 220 h the value of quadrupole-split of nanooxides (-0.009 - +0.079 mm/s) (at 78 K) does not differ from the value of quadrupole-split bulk oxides. It is not possible to compare the shape of the spectra because the sample das not contain enough iron oxide.

In [11] the size-dependent oxidation of thin iron was also studied. The Mössbauer spectra were obtained for various temperatures: 10 K < T < 300 K. Investigated particles had diameters in interval 50 - 200 Å. The authors established that the thickness of the oxidized shell of the iron particles is approximately equal to 12 Å. The spectra of the sample with a core diameter of 96 Å at temperatures of 4.2 K, 85 K and 300 K are presented in Fig. 17.

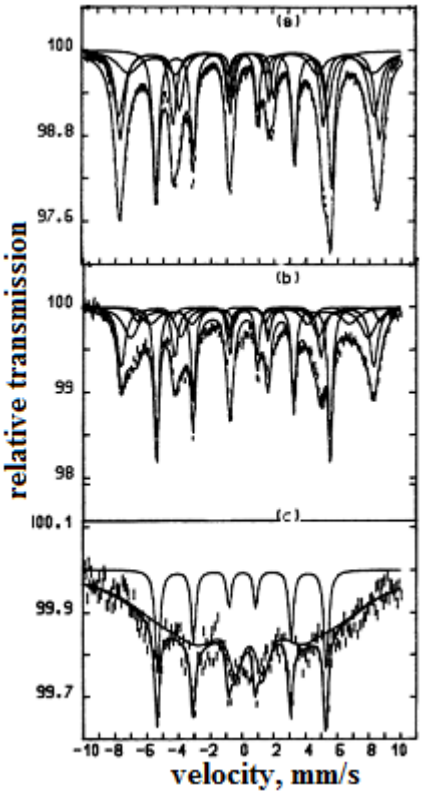

Fig. 17 The Mössbauer spectra of the sample having a core diameter of 96 Åat three temperatures: (a) 4.2 K (b) 85 K (c) 300 K [11].

It is clearly evident from the figure that the low-temperature spectrum is a superposition of several spectra with magnetic hyperfine structure from α-Fe and oxides. The components of this spectrum produce the Mössbauer parameters which can be attributed to Fe_3O_4 or γ-Fe_2O_3. Having assumed equal Debye factors, the authors obtained the ratio of the areas for metallic iron and the iron oxides (Table 10).

Table 10. Atomic portions of iron in oxide and metallic conditions.

Particle size (Å)	**wt. % Fe**	**wt. % Fe oxides**
275	41.6	58.4
214	27.8	72.2
113	30	70
100	16.5	83.5
88	7.3	92.7

At room temperature particles exhibit superparamagnetic behaviour which explains the broadening of the sextet lines for the iron oxide (see Fig. 17 c).
In another work [12] the oxidized and not oxidized ultrafine metal iron particles with average diameters of 2 nm were investigated. The Mössbauer spectra of particles with diameters of 2.4 ± 0.3 nm are presented in Fig. 18.

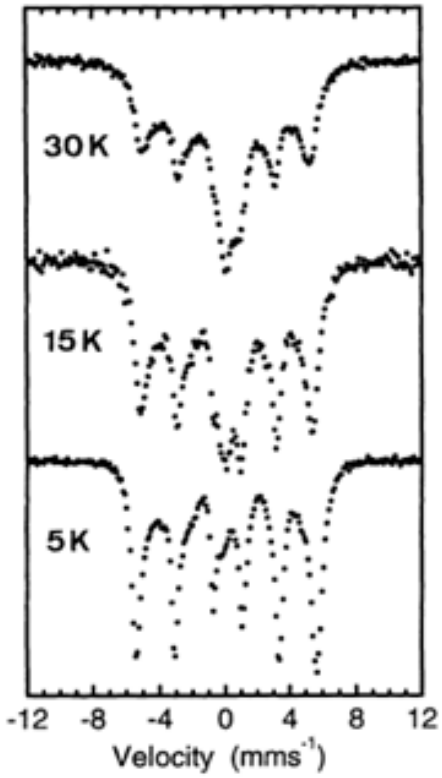

Fig. 18 The Mössbauer spectra of iron particles with diameters of 2.4 nm at various temperatures [12].

At 5 K the spectrum is similar to the spectrum of bulk α-Fe. This spectrum contains also a component of the hyperfine field 36 – 40 T which was assigned to surface atoms. Increasing the temperature to 30 K leads to a gradual broadening of the spectral lines and an increase of the absorption at zero velocity as a result of superparamagnetic relaxation. In Fig. 19 is shown the spectrum for oxidized (a) and not oxidized (b) iron particles (4 nm), obtained in the presence of an external field of 4.3 T; (c) is a residual spectrum. In the residual spectrum the component from α-Fe has been subtracted. The Mössbauer parameters are given in Table 11.

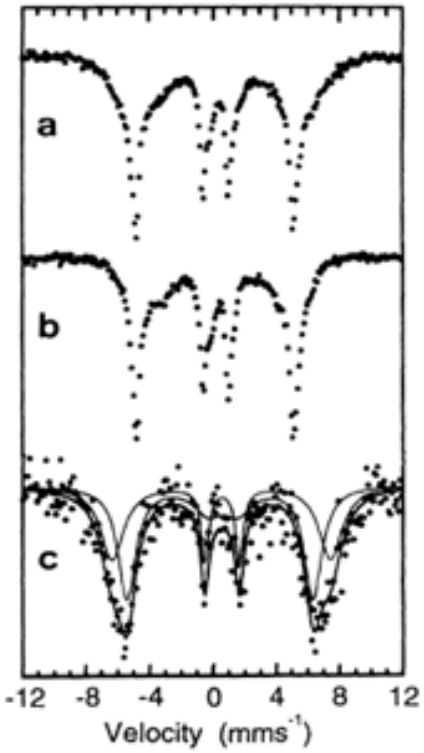

Fig. 19 The Mössbauer spectra of iron particles with diameters of 4 nm [12].

Table 11. The Mössbauer parameters of the oxide component of the iron particles with diameters of 4 nm [12].

		***IS*, mm/s**	***QS*, mm/s**	***B*, T**	**% ± 5 %**
Surface layer	***B* = 4.3 T**	0.56 ± 0.1	-0.01 ± 0.1	42.8 ± 5	46
		0.54 ± 0.1	-0.06 ± 0.1	36.5 ± 5	54
	***B* = 0**	0.44 ± 0.1	-0.04 ± 0.1	47.2 ± 5	44
		0.43 ± 0.1	-0.01 ± 0.1	41.2 ± 5	56
Full oxidation	***B* = 4.3 T**	0.51 ± 0.1	-0.01 ± 0.1	46.9 ± 5	58
		0.45 ± 0.1	-0.03 ± 0.1	41.4 ± 5	42
	***B* = 0**	0.48 ± 0.1	-0.02 ± 0.1	46.9 ± 5	57
		0.37 ± 0.1	-0.02 ± 0.1	41.7 ± 5	43

The disappearance the 2nd and the 5th spectral lines indicate a ferromagnetic ordering on the surface of the particles. In Fig. 20 the spectra of particles with

diameters of 4 nm without an external field (b) and in a field (a) were obtained at 5 K. The sample was measured after 26 hours of oxidation, when all iron had been oxidized.

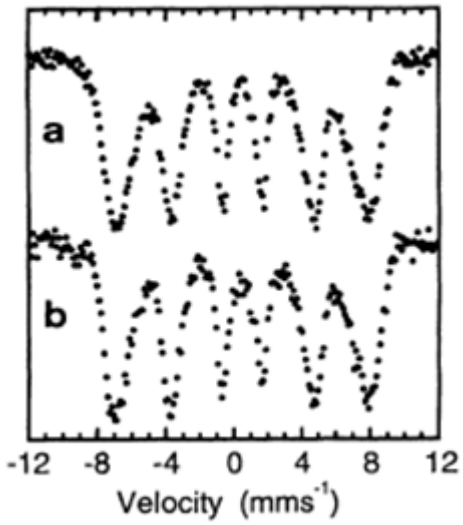

Fig. 20 The Mössbauer spectra of iron oxide, the diameters of particles d = 4 nm.

Apparently, the external magnetic field gives only rise to a line broadening. Also no splitting into two magnetic sextets for the fully oxidized particles in the magnetic field of 4.3 T was observed, contrary to spectra of bulk maghemite andstoichiometric magnetite. It was found earlier that on the surface of the oxidized particles of iron phases of Fe_3O_4 or γ-Fe_2O_3 with the spinel structure are formed. The authors [12] have assumed that the canted magnetic structure is due to the small sizes of the crystallites. It arises presumably because of the distribution of the «spin-canting» effect. Values of the Mössbauer parameters are presented in Table 11. Also the size of the hyperfine field is lowered in comparison with the bulk samples.

In [13] studied the evolution of the oxidation of ultrafine particles of α-Fe (with diameters of 5 nm) in an air atmosphere. Two sets of particles (A and B) were investigated. These sets differ by the preparation methods. From TEM data these particles consisted of a core and a thin oxidized film. The spectra of sample A, obtained directly after preparation, are shown in Fig. 21.

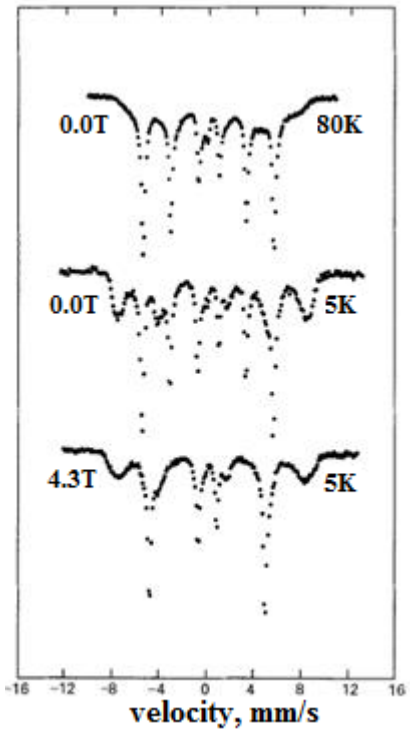

Fig. 21 The Mössbauer spectra of the sample A at 80 K in zero external magnetic field, and at 5 K in zero field and in a field of 4.3 T [13].

In the spectra the absorption lines from α-Fe and iron oxides are clearly visible. The relative area of the component from metallic α-Fe is approximately 48 % at 5 K (B_{HF} = 34.2 T, *IS* = 0.12 mm/s). At 80 K the area increases to 60 %. In the presence of an external magnetic field of 4.3 T, in the spectrum of α-Fe is observed a disappearance of the 2nd and the 5th lines of the sextet, while for the spectrum of iron oxide these lines remain visible. Simultaneously, for metallic iron, the size of the hyperfine field decreases to 30.2 T because the external magnetic field is antiparallel with the internal magnetic hyperfine field of α-Fe. Lines of the sextets from the iron oxide broaden at the presence of an external field, but the average values of the hyperfine fields (48 T and 50 T) and the relative areas (28 % and 20 %) remain constant. For the sextets the isomer shift is equal 0.4 mm/s. The spectra of sample A after the oxidation are shown in Fig. 22.

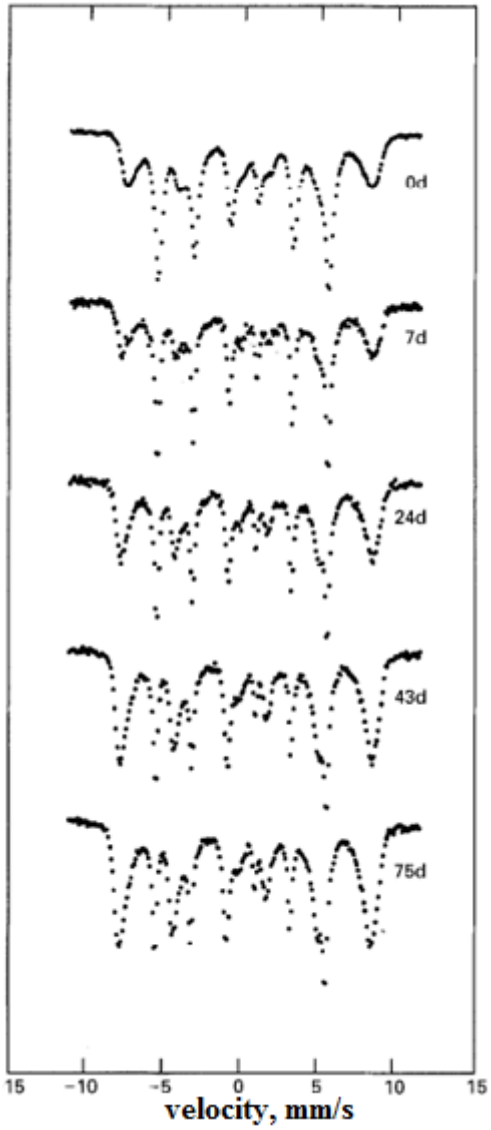

Fig. 22 The Mössbauer spectra of sample A after different oxidation times. All spectra have been obtained at temperature of 12 K [13].

As can be seen in Fig. 22 the content of iron oxide increases due to oxidation. For sample B the Mössbauer spectra are presented in Fig. 23.

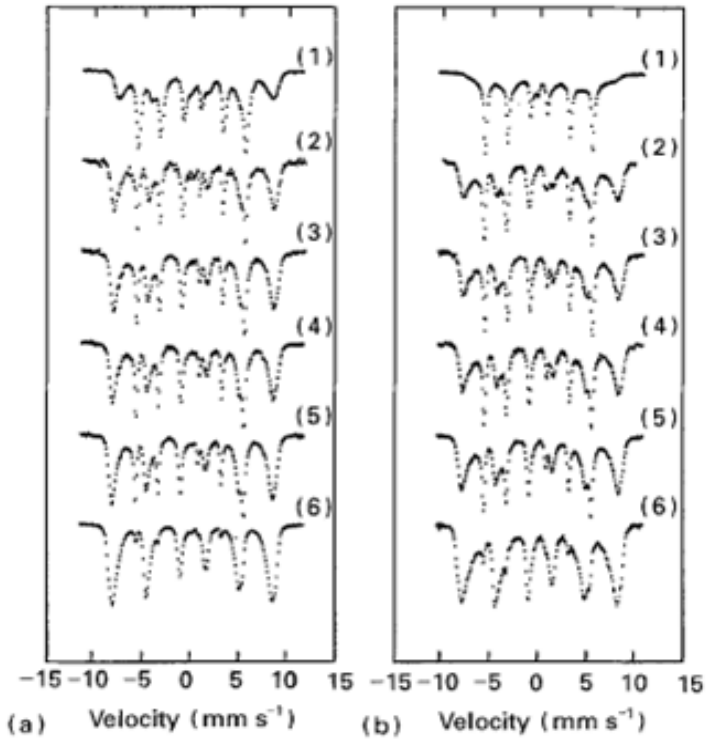

Fig. 23 The Mössbauer spectra of sample B after different oxidation times. Spectra (1) were measured from non-oxidized sample A; other spectra were measured from sample B oxidized for various times: (2) 0, (3) 1, (4) 2, (5) 4, and (6) 130 weeks. (a) Spectra measured at 12 K and (b) spectra measured at 80 K [13].

The values of the Mössbauer parameters are B_{HF} = 50.5 T, $IS \approx 0.47$ mm/s and the quadrupole splitting is insignificant for all spectra at 12 K. At 80 K B_{HF} = 48.5 T for B sample. In Fig. 24 is shown the dependence of the spectra of sample B on the temperature.

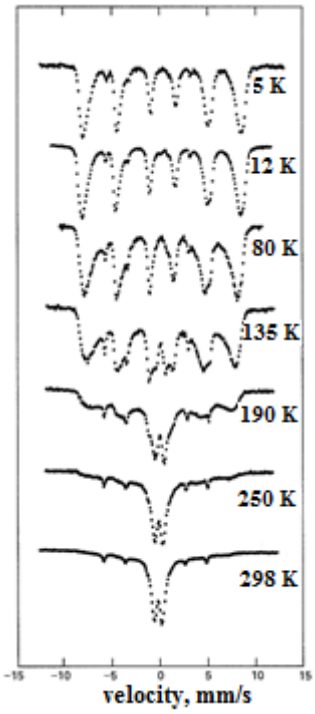

Fig. 24 The Mössbauer spectra of sample B at different temperatures. Oxidation time is 130 weeks [13].

It is seen that the magnetic splitting of the oxidized component of the spectra quickly decreases at 190 K. At 295 K the magnetic splitting almost completely collapses, unlike the component from α-Fe. Such behaviour of the spectra of nano-oxides (5 nm) differs from the spectra for the bulk oxides. Magnetic splitting remains at room temperature for the spectra of the bulk oxides. Measuring the sample with a magnetic field of 0.6 T shows that the collapse of the magnetic splitting is a consequence of superparamagnetic relaxation, instead of a transition into the paramagnetic state. From the average value of the hyperfine field (48.0 T - 50.5 T), it is possible to conclude that the oxidized layer represents a mixture of Fe_3O_4 and γ-Fe_2O_3. The authors [13] obtained the Verwey transition between 12 K and 80 K. They explained the reduction of the Verwey temperature by the small particle sizes and the nonstoichiometry of magnetite.

In [14] the investigation of oxidized particles of iron was continued. The surface layer of the investigated particles consists of small iron oxide clusters. The surface layer is reconstructed as a result of annealing, and big clusters of high-quality stoichiometric magnetite with a Verwey temperature of 120 K are

formed. Two sets of particles with the identical sizes of cores and surface layer thickness were investigated. The sets differed in the degree of oxidation and microstructure of the surface layer. Though the oxidation layer around a metal core impedes further oxidation, the authors [14] have shown that it cannot suppress the oxidation process completely as in was shown in work [13]. The investigated particles were almost spherical form, with diameters of $\langle D_1 \rangle \approx 14.9$ nm for sample I and $\langle D_2 \rangle \approx 15.2$ nm for sample II. The Mössbauer data was measured in the temperature interval of 4 – 300 K and examples of spectra are shown in Fig. 25.

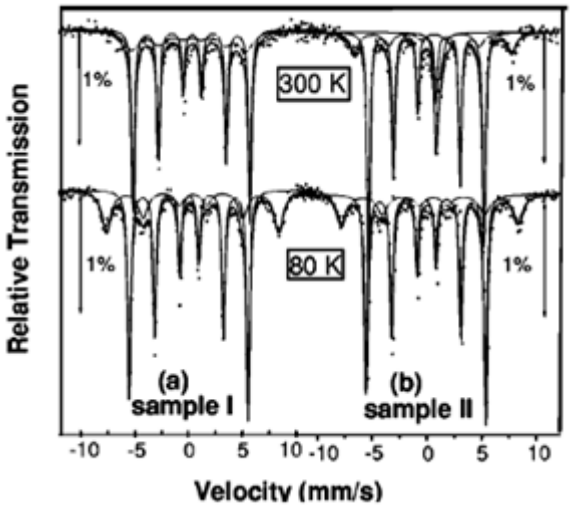

Fig. 25 The Mössbauer spectra at 300 K and at 80 K for samples I and II [14].

The presented spectra can be analyzed with two magnetically split subspectra area ratios of 65:35 %.

For both samples the more intense sextet with the narrow lines can be attributed to the body-centered cubic (bcc) iron (same as α-Fe). At 80 K the hyperfine field of α-Fe component is B_{HF}(Fe) = 34 ± 0.3 T. The second sextet has a larger field of 49.6 ± 0.3 T and can be attributed to the oxide phase. As is apparent from the figure, at room temperature, the magnetic splitting for the oxide components is retained for the sample, which has a larger particle size. This was not observed for the sample consisting smaller particles (see above). The value of the hyperfine field (49.6 ± 3 T) at 80 K remains lowered in comparison with the field for volume magnetite (51.5 T). In view of the Mössbauer resonant areas for both

components, and considering the difference of density of Fe (7.87 $g \cdot cm^{-3}$) and Fe_3O_4 (5.18 $g \cdot cm^{-3}$), the authors have found that for the particles with the diameter of 15 nm the average thickness of the oxide film is approximately 1.7 nm. In the spectra of sample II a third component appears at 300 K. This component is a paramagnetic doublet with a resonant area equal to 10 %, IS = 1.06 mm/s, and QS = 0.44 mm/s. The paramagnetic doublet can be attributed to the FeO phase. In the spectrum of sample I also at 300 K the subspectrum of iron oxide shows a relaxation behavior with slightly broadened peaks and with a decrease of the hyperfine field to 33 T. The value of 44 T was found for this component for the sample II. The authors [14] have attributed such behavior to the presence of temperature-dependent fluctuations in the oxide shell of particles at lower temperatures the fluctuations are blocked. From the behavior of spectrum I and from the results obtained in earlier works, the authors have concluded that the surface layer (1 - 2 nm) of iron particles consists of very small oxide clusters with enter the superparamagnetic state with increasing temperature, and the strong «spin-canting» effect.

Also, a step change of magnetization is observed in sample II near 122 K (see Fig. 26).

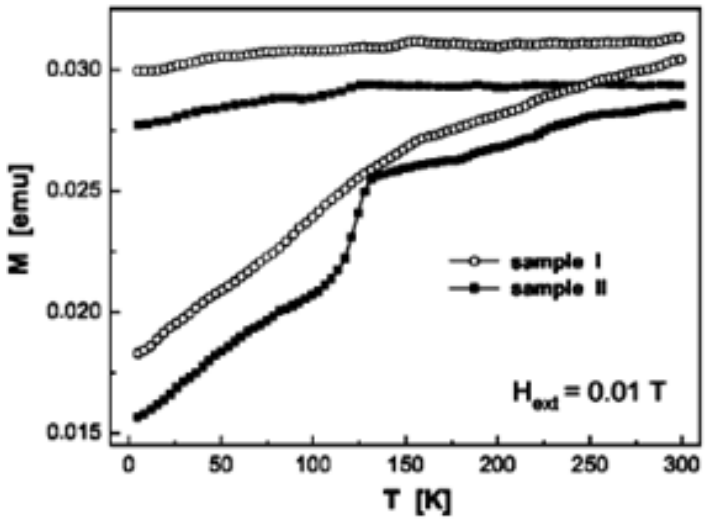

Fig. 26 Temperature dependence of ZFC-FC magnetization curves [14].

This change has allowed to determine the Verwey temperature in the shell of annealed magnetite particles. The Verwey temperature coincides with the

Verwey temperature for volume samples which is equal -150°C (123 K). On the other hand, the lack of this sharp transition in sample I confirms that the surface layer of the particles of this sample consists of small nonstoichiometric clusters of iron oxide for which the Verwey transition is observed at the lower temperature of 12 – 80 K, as shown in [13]. A sharp transition observed in sample II at the Verwey temperature, clearly indicates that the thin surface layer of these particles consists of high-quality stoichiometric magnetite.

Summary of chapter 2.2.1

Thus, considering the above investigations of iron nano-oxides and comparing the results to bulk parameters, it is possible to draw following conclusions:

1. The small particles of nano-oxide (less than ~ 10 nm) have magnetically ordered state at low temperature. At transition to room temperature the spectra exhibit the doublet that was explained by the superparamagnetic state of these particles. But in the bulk samples the magnetic splitting remains at room temperature.

2. By increasing the particles size (up to 15.4 nm), the magnetic splitting in the spectra is retained for the oxide component of the Mössbauer spectra, recorded at room temperature.

3. Also, for small particles of iron oxide (less than ~ 10 nm) a reduction of the hyperfine fields experienced by the iron nuclei in comparison with volume values is characteristic.

4. For magnetite, a decrease of the Verwey temperature is observed. The experimental value is between 12 and 80 K, whereas for the volume oxides T_v = -150°C (123 K).

2.2.2. Iron oxide nanoparticles

At the present time, nanoparticles are defined as objects with size from 1 to 100 nm. To nano-objects include solid-state clusters, nanostructures and matrix nanoclusters. Such nanostructures can be obtained in various ways (photochemical reactions, mechanochemical ways, et cetera). By mechanochemical synthesis it is possible to obtain nanoclusters that are isolated from each other. Also it is possible to influance in a clusters size, cluster interaction, intercluster interaction and interaction between cluster and matrix using the size and surface properties of pores.

In 1970 appeared first Mössbauer spectroscopy works that were devoted to research of fine-dispersed powders of iron oxide. In [15] studied powder of magnetite with particle sizes 400 Å. They obtained experimental spectra which are in contradiction with typical earlier spectra of bulk magnetite (see Fig. 27). The authors measured the spectra of magnetite, undergone to oxidation by air at room temperature (Fig. 28).

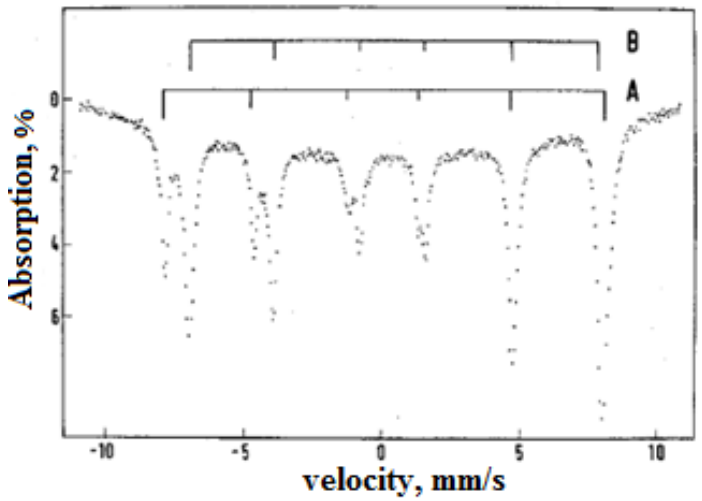

Fig. 27 The Mössbauer spectrum of Fe_3O_4 at 298 K [15].

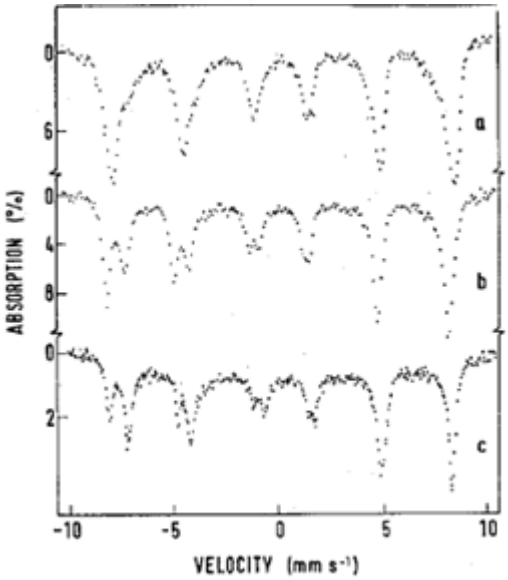

Fig. 28 The Mössbauer spectra of magnetite nanoparticles after oxidation (80 days) a) and b); c) sample b) treated at 700 K with CO_2/CO mix.
The spectra were measured at room temperature [15].

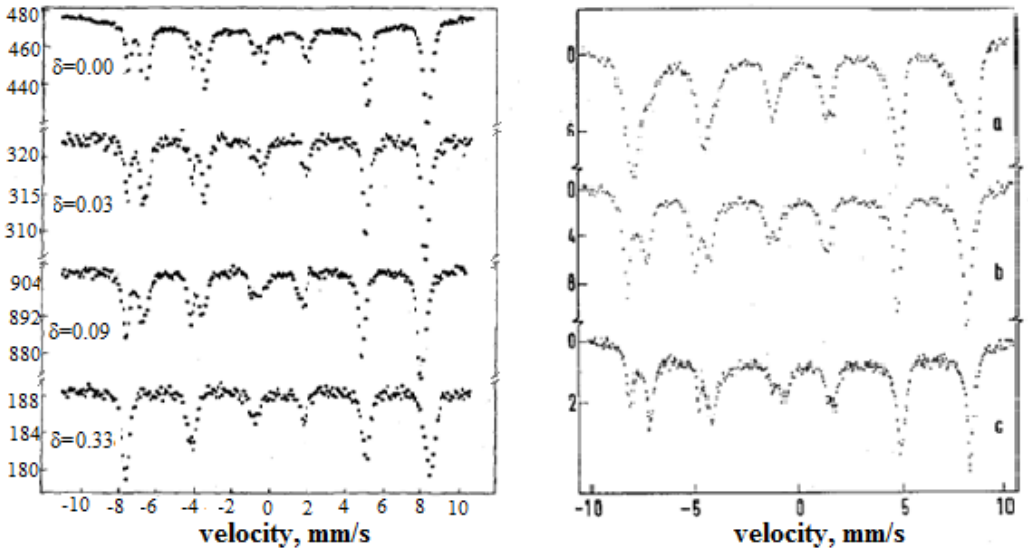

Fig. 29 The Mössbauer spectra of magnetite. Spectrum of bulk magnetite $Fe_{3-\delta}O_4$ at 296 K with various stoichiometry (left), spectrum of two different magnetite samples (d = 400 Å) (right) [15, 16].

In Fig. 29 (on the right part) is shown the spectra of two different magnetite (both 400 Å), after oxidation at room temperature. In both spectra the ratio between the spectral areas (for octahedral sites and tetrahedral sites of iron ions) was below 2 (the values for stoichiometric magnetite). Reconstruction of

stoichiometric magnetite was observed when treating of magnetite by mix CO_2/CO (S = 2, Fig. 27). From behavior of the spectrum at oxidation of samples it was concluded that investigated samples are nonstoichiometric, namely the existence of solid solution of Fe_3O_4 - γ-Fe_2O_3. Also anther spectra (see [16] and Fig. 29) confirm this conclusion about the nonstoichiometric samples. In Fig. 29 the ratio of spectral lines changes with size of δ.

In [17] investigated dependence between the particle sizes and the structure of γ-Fe_2O_3. These particles were made from thin dispersed crystallites. The investigation was based on presence of 2^{nd} and 5^{th} lines at the Mössbauer spectra of ^{57}Fe with application of external magnetic field. Being based on earlier results [18, 19], the authors assumed that for the particles, which have the size lesser than 10^4 Å, a canted spin structure is typical on the surface of these particles. To prove this, the Mössbauer spectra of spherical particles of pure maghemite were measured. The sizes of the particles were 10^2 - 10^3 Å and the sizes of crystallites were from 70 Å to several hundred angstroms. The spectra were measured at the temperature 4.2 K with an external field of 5.0 T. The obtained spectra of four maghemite samples with the various sizes are presented in Fig. 30.

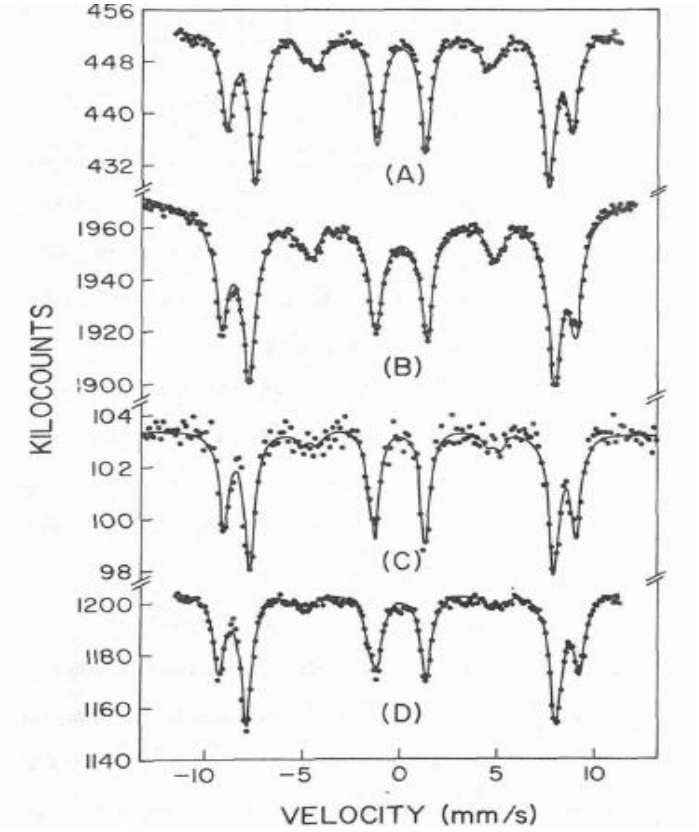

Fig. 30 The Mössbauer spectra of maghemite with the various sizes [17].

From the amplitude ratio of 2nd and 5th spectral lines and 1st and 6th lines the authors estimated the thickness of spin-canted layer at the surface of the particles. Results are given in Table 12.

Table 12. The parameters of maghemite particles with the various sizes [17].

Sample	**Particle size (Å)**	**Crystallite size (Å)**	**$A_{2,5}$ (A, B)/$A_{1,6}$ (A, B)**	**Canted-layer thickness (Å)**
A	65	70	0.213	5
B	175	97	0.127	4
C	300	207	0.137	7
D	955	303	0.091	7

These results were confirmed by authors of a former work [20] (see Fig. 31) where was investigated cubic iron oxide particles with the crystallite diameters of ~ 27 Å, generated on surface with areas of ~ 293 Å. In the obtained spectrum

a large spin-canting effect was observed. The ratio of the areas of 2nd, 5th and 1st, 6th lines was 0.690. This indicated that a canted spins occupy whole crystallite.

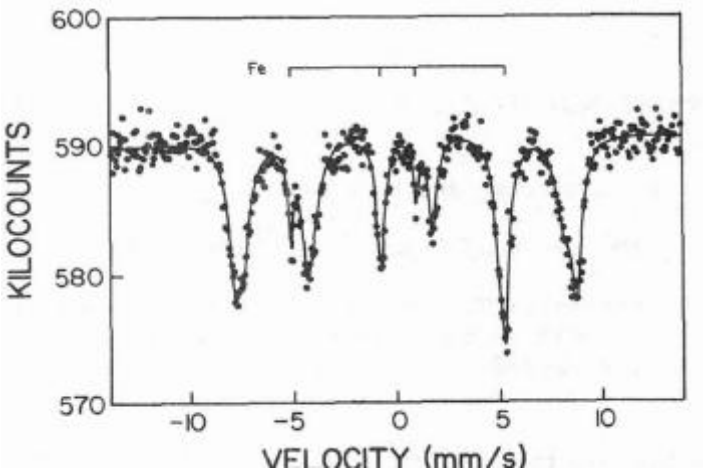

Fig. 31 The Mössbauer spectrum of the oxidized powder of iron in the external parallel magnetic field of 2.5 T at the temperature 4.2 K [20].

Using the obtained results, authors assumed that the crystallites are divided by magnetic grain boundaries in which the surface spins undergo of cant. Also, authors concluded that the crystallites have more important influence on the spin-canting effect, than the size of the particles. Thus, morphology of the particles is a critical factor, influencing on the magnetic properties of these particles.

Besides these results, in Fig. 30 it is clearly visible that the spectrum of maghemite, in an external magnetic field 5.0 T, is superposition of two subspectra unlike the known spectra of volume and nanomaghemite in zero magnetic fields. It indicates a ferromagnetic structure of this material below Curie temperature.

In [21] was obtained Mössbauer spectra of magnetite nanoparticles. Their diameter was calculated by authors and was equal 8 nm. The investigation was done using the superdispersed powder of magnetite, obtained by standard chemical condensation method. At room temperature the Mössbauer spectrum of magnetite nanoparticles (see Fig. 32) conformed to the spectrum of bulk sample below the Verwey temperature.

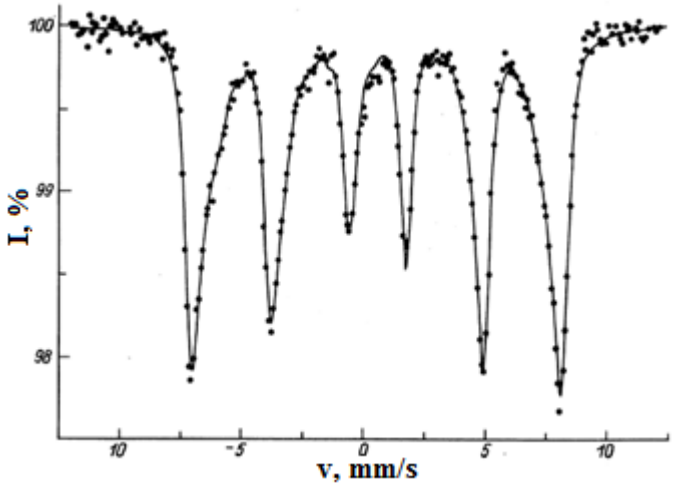

Fig. 32 The Mössbauer spectrum of magnetite nanoparticles at 300 K [21].

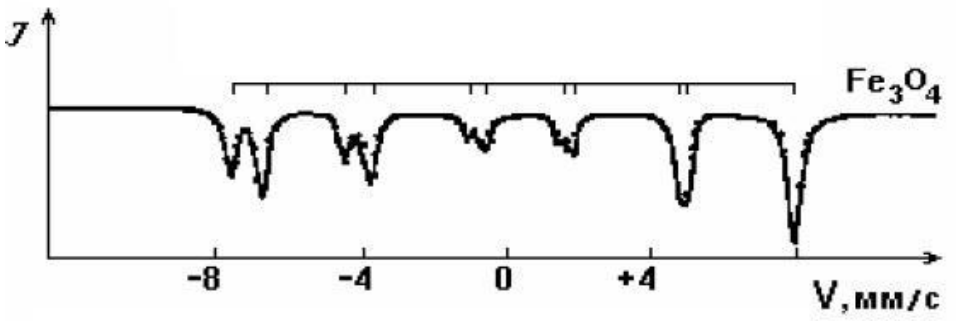

Fig. 33 The Mössbauer spectrum of bulk magnetite, T = 300 K [7].

Considering that the spectrum of bulk magnetite at room temperature looks like two magnetic sextets (see Fig. 33) and comparing the spectrum to the spectra in Figs. 28 and 29, it is possible to conclude that authors dealt with nonstoichiometric magnetite samples.

The authors considered this spectrum as superposition of three partial spectra corresponding to trivalent atoms of iron in A and B sites and to bivalent atoms of iron in B site. From distribution function of effective magnetic fields four values of fields were defined: B_{n1} = 40.7 T, B_{n2} = 43.1 T, B_{n3} = 45.6 T and B_{n4} = 48.2 T. Last two field values were carried to the ions of bivalent iron, and also to the ions of trivalent iron in the A and B sites which was included in the internal areas of the particles. The B_{n1} and B_{n2} fields were considered similar to B_{n3} and B_{n4}, concerning the ions in "surface" area of the particles. Reduction of values of "surface" fields on ~ 5.0 T was explained by various numbers of

indirect exchange coupling for "internal" and "surface" ions of iron. The values of the hyperfine field 48.2 T and 45.6 T coincide with field values of bulk samples.

In [22] nanoparticles of iron oxide (namely magnetite) were investigated in temperature interval from 4 K to room temperature. These particles had the sizes 7 nm and 13 nm. Besides the basic magnetite phase the fit of the low-temperature spectra of 7 nm and 13 nm particles showed also inclusion of hematite or goethite. As a whole, however, the spectra look typical spectra for magnetite below the Verwey temperature. The obtained values of hyperfine fields for 7 nm particles were approximately 1 T less in comparison with the value for the sample having the size 13 nm. Authors explained this result by the collective magnetic excitation effect in small magnetic domains. A collective magnetic excitation effect reduces the observable hyperfine field in comparison with the bulk material. For 13 nm sample the obtained spectrum at 170 K was compared with the spectrum of magnetite at room temperature. As evident from the obtained spectrum (see Fig. 34), in the experimental spectrum is clear division of the spectrum into two sextets: A and B (clear distinction in isomer shifts for A and B positions). Authors explain this by the nonstoichiometric structure of investigated sample. Using the data about isomer shifts, authors have come to conclusion that it is possible to present the investigated material as the mixture of 32 % of maghemite (γ-Fe_2O_3) dna 68 % of magnetite (Fe_3O_4).

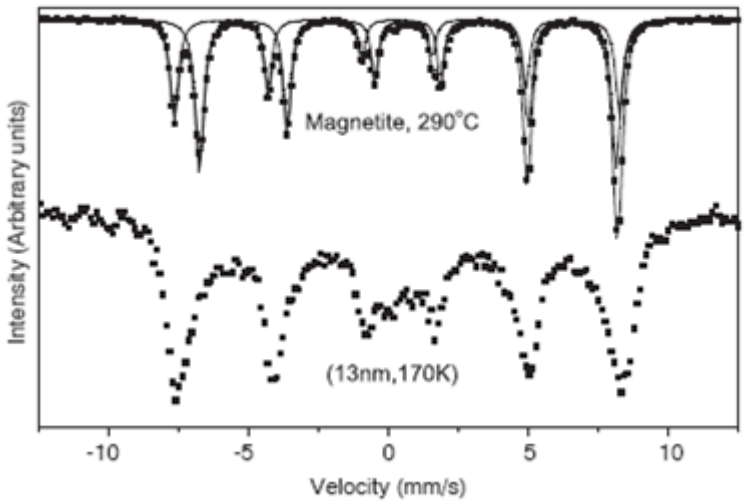

Fig. 34 The Mössbauer spectra for magnetite particles with diameter of 13 nm, and the spectrum of magnetite above the Verwey temperature [22].

In [23] was studied a number of the samples prepared by the thermal decomposition method. The samples contained particles of maghemite, having spherical form with diameter of 4 nm and 12 nm, and the cubic form with edge of 9 nm. Measuring the Mössbauer spectra as a function of temperature (see Fig. 35) authors have found out that the particles show behavior characteristic for magnetic single-domain particles. Besides, authors find out a superparamagnetic behavior at high temperatures.

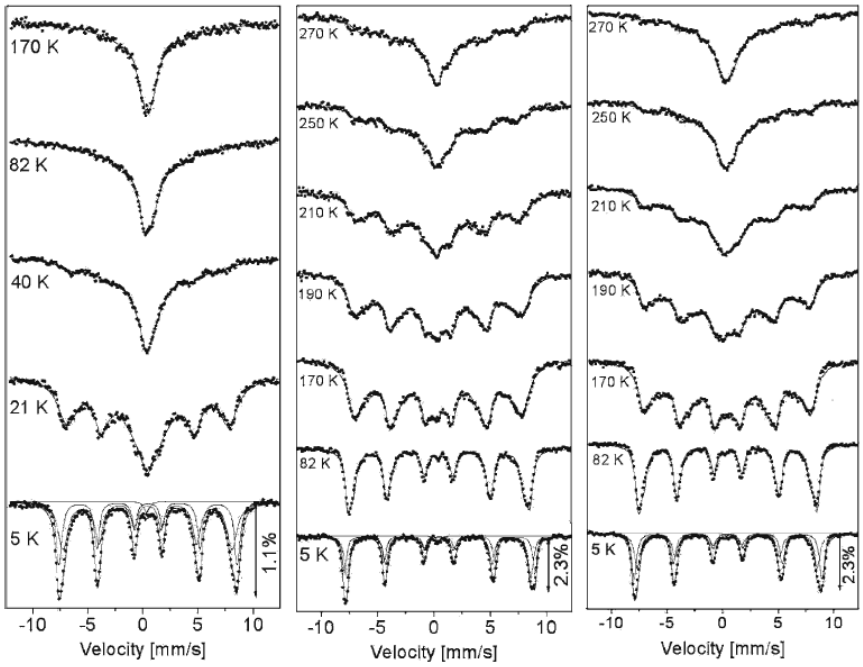

Fig. 35 The Mössbauer spectra of maghemite. From left to right: sample I (spherical 4 nm particles), sample II (spherical 12 nm particles) and sample III (cubic 9 nm particles) [23].

At the temperature 5 K the spectra of all samples showed pure magnetic sextet. Parameters of the spectra are resulted in Table 13.

Table 13. The Mössbauer parameters of the sample I, II and III at 5 K [23].

Sample	***IS*, mm/s ±0.005**	***QS*, mm/s ±0.01**	***B*, T ±0.05**	***Γ*, mm/s ±0.01**
I	0.442	0.00	48.76	0.55
II	0.440	0.00	51.31	0.49
III	0.443	0.00	51.31	0.58

In comparison with the bulk sample values, authors explained the lowered hyperfine fields by collective magnetic excitation effect and surface effects. With increasing the temperature the width of spectral lines increase and typical superparamagnetic behavior was detected. In addition to decreasing of the effective magnetic field as the dimensional effect, authors also found out increase of the anisotropy constant with decreasing of the particles size. Also on spectra (see Fig. 35) of the 4 nm diameter particles the lines broadening is

observed at 5 K in comparison with larger particles. Though the spectrum has been approximated by two sextets, obvious separation of the spectrum is not observed.

A ferromagnetic ordering of the maghemite nanoparticles with diameter 14.5 nm for spherical particles and with 12 nm edge for cubic particles was observed in [24]. The spectra were measured with application of the magnetic field 5.5 T perpendicular to direction of gamma-rays.

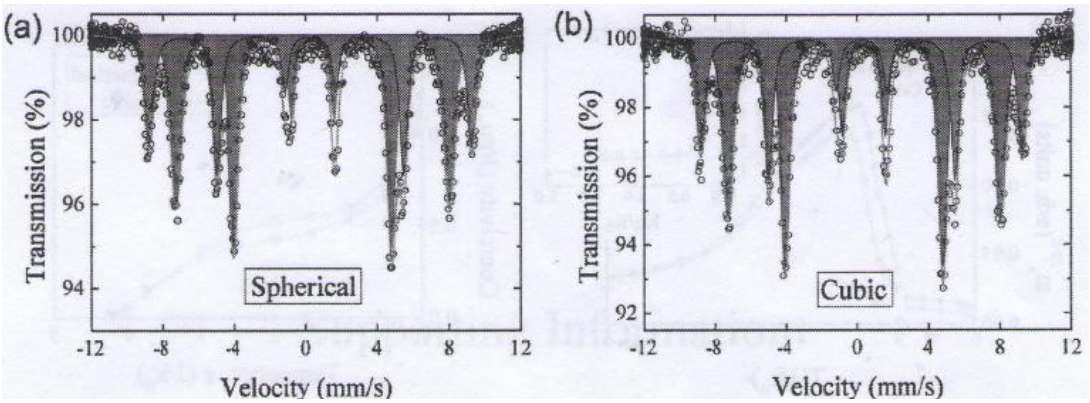

Fig. 36 The Mössbauer spectra for spherical (a) and cubic (b) particles in field of 5.5 T and T = 5 K [24].

Apparently from figure, at presence of the magnetic field of 5.5 T the spectra are completely resolved. Two observed sextets of lines correspond Fe^{3+} cations in the tetrahedral and the octahedral sites.

Summary of chapter 2.2.2

It is possible to draw the following conclusions for the completely oxidized iron nanoparticles:

1. The shape of the Mössbauer spectra of the investigated samples at similar temperature depends on the size of the investigated particles and the stoichiometric structure of material (for the magnetite).

2. For the particles that are located in the surface layer of investigated substance, and also for the majority of particles with the small size, decreasing of hyperfine magnetic field on iron nuclei is observed in comparison with bulk samples.

3. The spectra of maghemite split on two sextets in an external magnetic field are observed. This is connected with ferromagnetic ordering of maghemite below the Curie temperature.

2.2.3. Clusters of iron oxide in matrices

Matrix nanoclusters and nanosystems represent the most common nanosystems in the nature. Stabilisation of nanoclusters in a matrix allows one to study nanoparticles which have different types of interactions both with the matrix, and between the clusters. For example, matrix isolation of nanoclusters allows one to observe new dimensional effects for isolated clusters. In this part of the thesis will be considered some investigations by nuclear gamma resonance spectroscopy of iron oxide nanoclusters in various matrices.

In [25] hematite nanoparticles in a TiO_2 matrix were studied. The size of the hematite particles in the matrix varies from 4 nm to 10 nm. The Mössbauer spectra of these samples contained paramagnetic and superparamagnetic doublets. The isomeric shift was 0.34 mm/s for the superparamagnetic doublet of the sample with particle diameter of 6.2 nm. By examining the spectra of samples with various particle diameters, the authors have concluded that the nanoparticles start to show superparamagnetic behavior in the case of hematite. It is the result of size reduction of the investigated particles to less than 10 nm. When the diameter is more than 10 nm (in SiO_2 - Fe_2O_3 [26]), nanoparticles of hematite show normal ferromagnetic behavior.

By 2001 appeared works [27, 28] devoted to the synthesis of isolated nanoclusters and nanosystems and investigations of their new properties, connected with dimensional cluster effects and intercluster iinteractions.

Mössbauer spectroscopy was used for determination of the cluster size of synthesized nanosystems, and also for the research on magnetic phase transitions and determination of the critical cluster sizes at which the change of magnetic properties of the cluster take place.

Two cluster systems were investigated: weakly and strongly interacting clusters.

System 1 is a system of clusters with weak interaction and with cluster sizes of R_{max} = 5 - 6 nm; system 2 is a system with strong interaction and with cluster sizes of R_{max} = 10 - 25 nm.

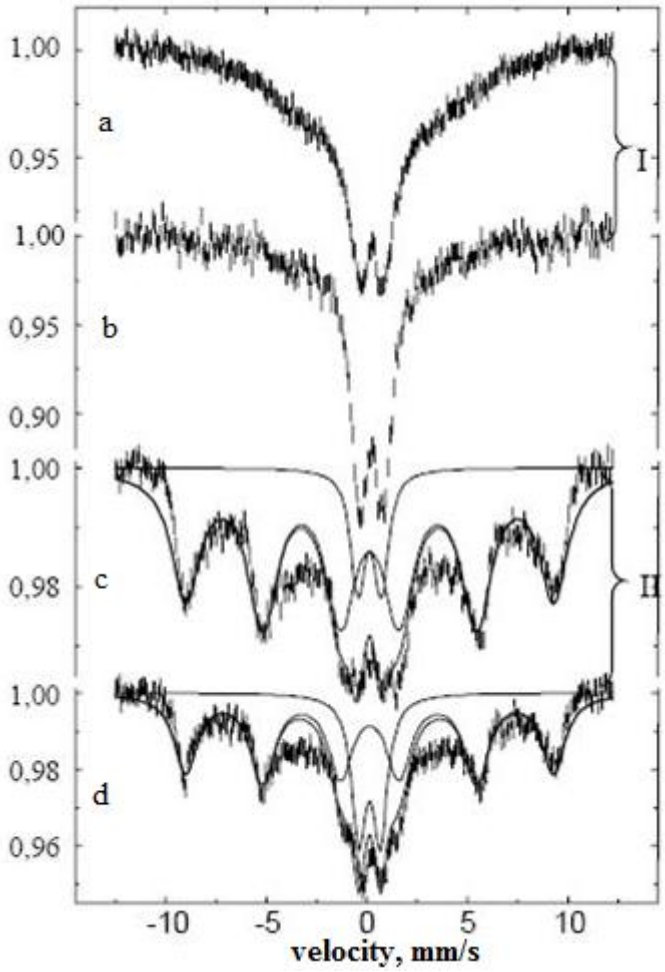

Fig. 37 The Mössbauer spectra of systems 1 and 2 [27].

In Fig. 37 the Mössbauer spectra of systems 1 and 2 are presented. Smearing of the magnetic superstructure in the spectra (Fig. 37 a, b) in system 1 indicates the occurrence of superparamagnetism that is a consequence of thermal fluctuations of the magnetic moment of the cluster as a whole. In Fig. 37 (c, d) is shown the spectra of system 2 with a resolved magnetic hyperfine structure and a narrow central paramagnetic doublet.

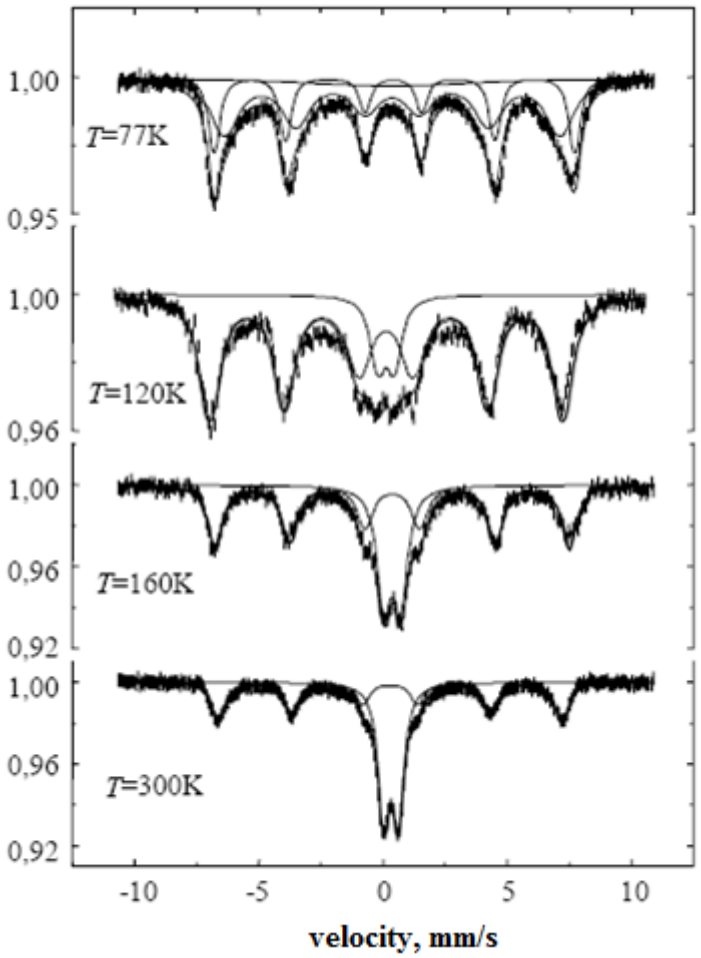

Fig. 38 The Mössbauer spectra of a nanocluster system of α - Fe_2O_3 - γ-Fe_2O_3 [28].

The Mössbauer spectra of the α – γ - Fe_2O_3 system (Fig. 38) indicate presence of a discontinuous magnetic transition between a magnetically ordered state with a characteristic hyperfine structure and a paramagnetic state, of which the central doublet is a proof. These magnetic transitions occur at 120 – 300 K and are connected with the "strong" intercluster interaction in the α – γ - Fe_2O_3 system.

In [29] the sizes of the iron oxide particles in the mesoporous SiO_2 matrix were studied. The sample contained mixture of hematite and maghemite particles. The size of the magnetic field (B = 51.5 ± 0.5 T) indicated that the sizes of the hematite particles was more than 15 nm whereas for maghemite the field had a lower value of B = 48.4 ± 0.5 T in comparison with bulk materials. The size of particles was 5 - 8 nm.

In [28] was applied Mössbauer spectroscopy (Fig. 39) for determining the structure of synthesised clusters.

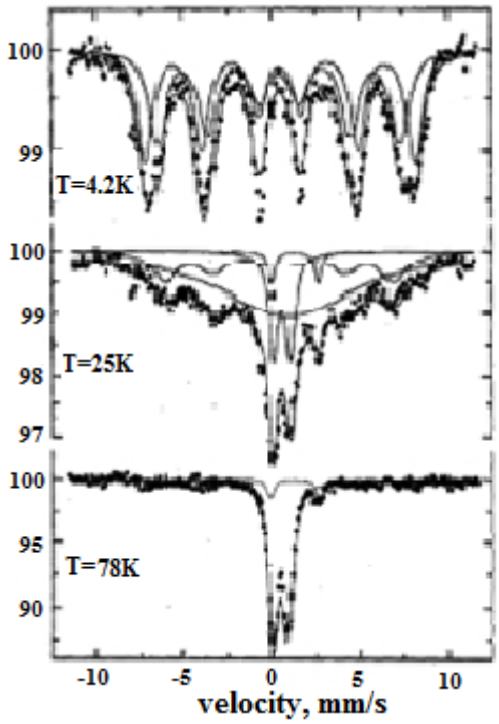

Fig. 39 The Mössbauer spectra of a nanostructure containing the iron oxides nanoclusters at different temperatures [28].

At 4.2 K the spectrum shows a magnetic hyperfine structure which is characteristic for γ-Fe_2O_3. The spectrum consists of two sextets, which the authors connected to atoms on the surface and inside the cluster. With increasing temperature the authors observed smearing of the spectral structures which is characteristic for superparamagnetic behavior.

Summary of chapter 2.2.3

The following conclusions can be made:

1. For matrix nanoclusters, and for completely oxidized iron particles, decreasing the cluster size leads to decreasing of the hyperfine magnetic field acting on the iron nuclei in comparison with bulk materials.

2. By decreasing the investigated cluster sizes below 10 nm, the iron oxide starts to show superparamagnetic behavior. Particles larger than 10 nm exhibit a behavior that corresponds to a magnetically ordered state.

3. For larger cluster sizes (20 - 50 nm) was observed discontinuous magnetic transitions between a magnetically ordered state with a characteristic hyperfine structure, and a paramagnetic state, characterized by a paramagnetic doublet.

Chapter 3. Experiment and discussion

3.1. Available samples

In this work several samples of γ-Fe_2O_3 were studied. The samples contained nanoparticles with various diameters and had different shapes: spherically shaped particles with a diameter of 20, 14 and 9 nm and cubic particles with an edge length of 9 nm.

Samples were synthesized by a method of thermal decomposition (Stockholm University, Sweden) [30]. Monodisperse iron oxide nanocrystals were produced using a surfactant-free thermal decomposition of the iron alkoxide route with addition of oleic acid and without it. This method yields iron-oxide nanocrystals of well-defined shape and size. The size and the shape of the nanoparticles can be controlled by the heating rate and the ratio between additional oleic acid and the iron containing reactant. The size of the samples was measured by transmission electron micrographs (TEM).

Mössbauer spectra of four different iron oxide nanoparticles with various size and shape were collected.

3.2. Studies

The spectra of the smallest and largest nanoparticles of maghemite (γ-Fe_2O_3) were obtained at 300 K and 77 K. These Mössbauer spectra were measured in the Physics Department of Åbo Academy (Turku, Finland) with Dr. Johan Linden. Results are represented in Fig. 40.

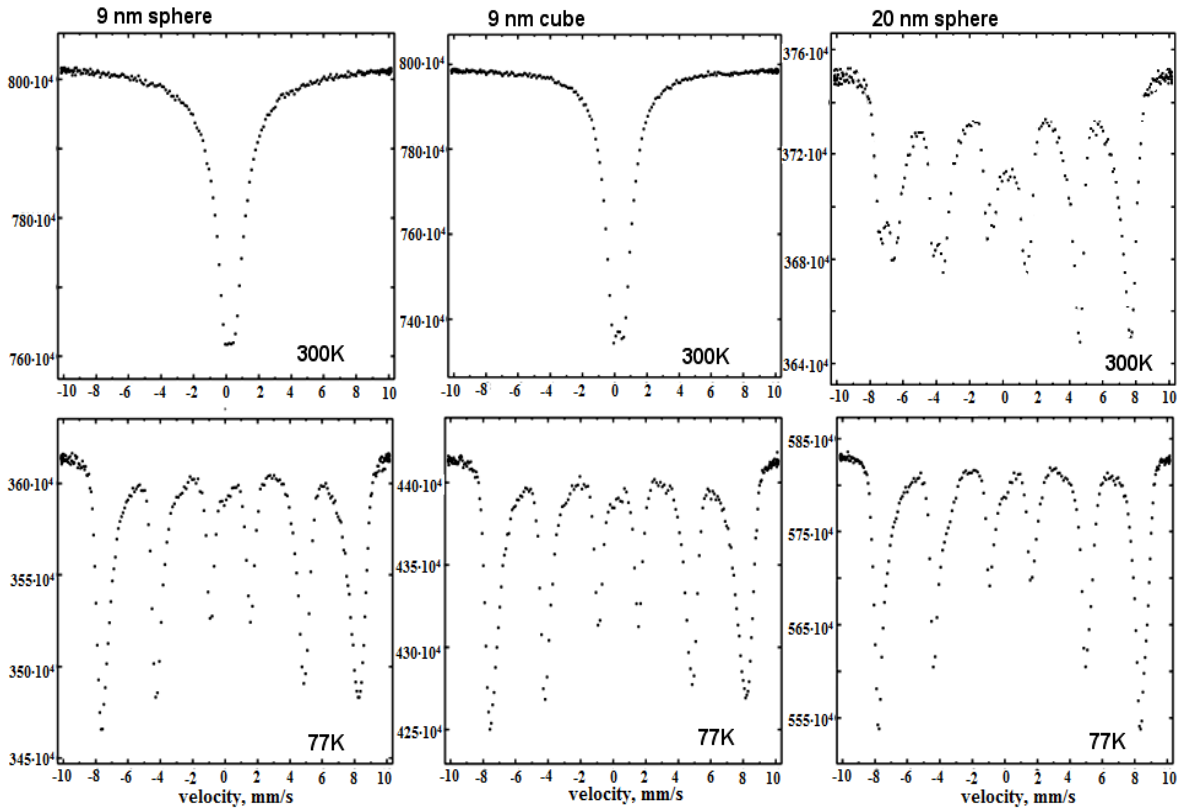

Fig. 40 The Mössbauer spectra of maghemite nanoparticles with diameters of 9 nm and 20 nm at different temperatures.

It is clear that at 77 K these spectra look like the spectra of the bulk materials.

The Mössbauer spectra show that all investigated samples have magnetically ordered structure at this temperature, independent of the size of the particles. At room temperature a clear difference from the bulk material spectra is seen already for the 20 nm particles in which a splitting into two components is observed. Also, at 300 K, with reducing the size of the particles, the nano-oxides of iron start to show superparamagnetic behavior. It is seen a broadening of the spectral lines and loss of the hyperfine structure leading to an increase of spectral intensity in the centre, followed by a total disappearance of the magnetically ordered structure.

The Mössbauer spectra of other nanoparticles of maghemite were measured in the Mössbauer laboratory of Saint Petersburg State University (see Figs. 41 and 42). These nanoparticles are spherical particles of maghemite with an intermediate diameter of 14 nm from the same series of samples.

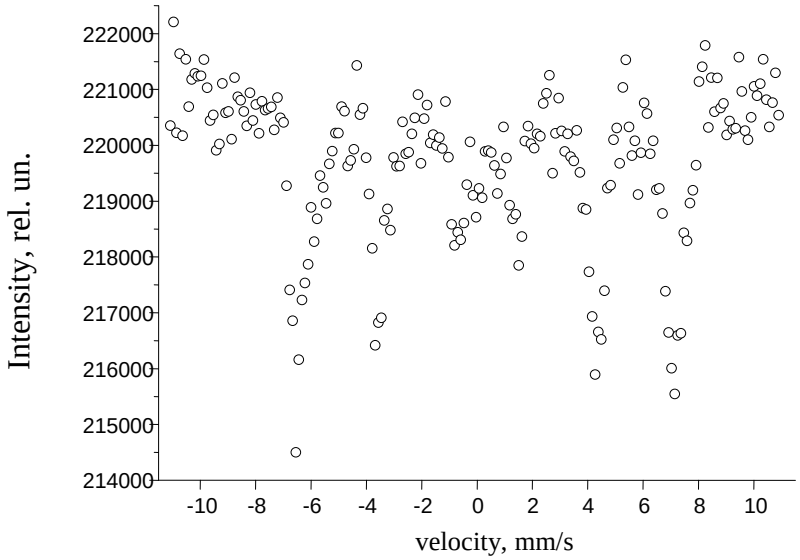

Fig. 41 The Mössbauer spectrum of 14 nm maghemite nanoparticles at 78 K.

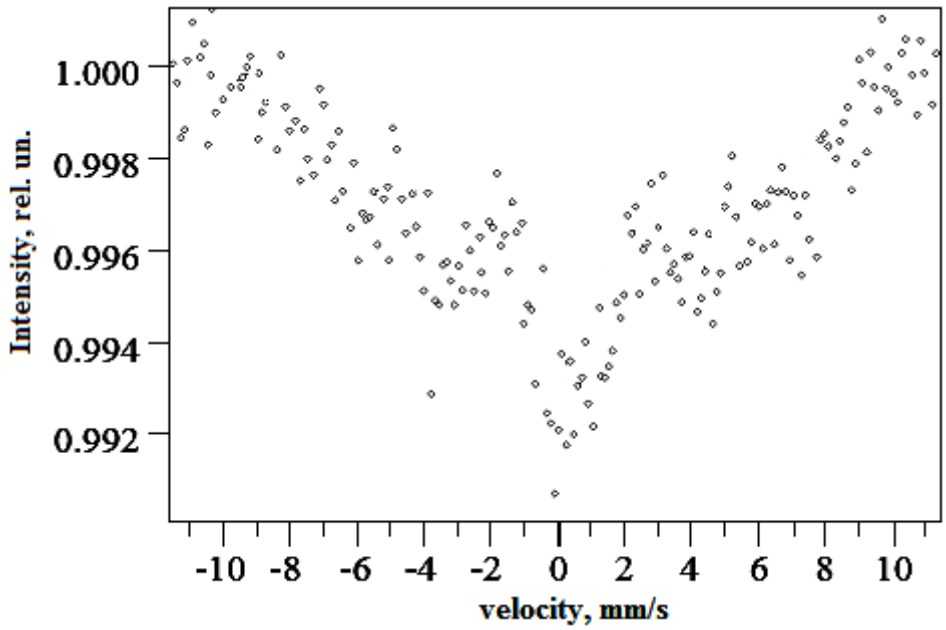

Fig. 42 The Mössbauer spectrum of 14 nm maghemite nanoparticles at 300 K.

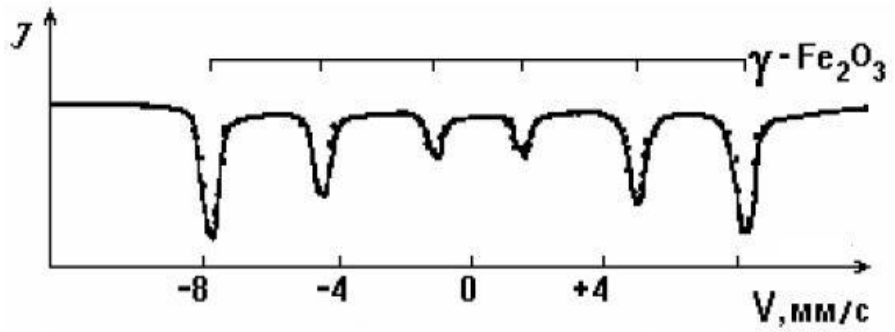

Fig. 43 Spectrum of bulk maghemite at 300 K (from literature [7]).

Also for the other samples of this series, a magnetically ordered structure was found at liquid nitrogen temperature. At room temperature, in comparison with the bulk material, our spectra show relaxation behavior. The spectral lines are strongly broadened and the subspectra are indistinguishable. It is obvious that at room temperature a paramagnetic component appears.

Next we make a decomposition of the spectra into components using the software Fit_programm (for spectra obtained in Russia) and MossWinn (for spectra obtained in Finland).

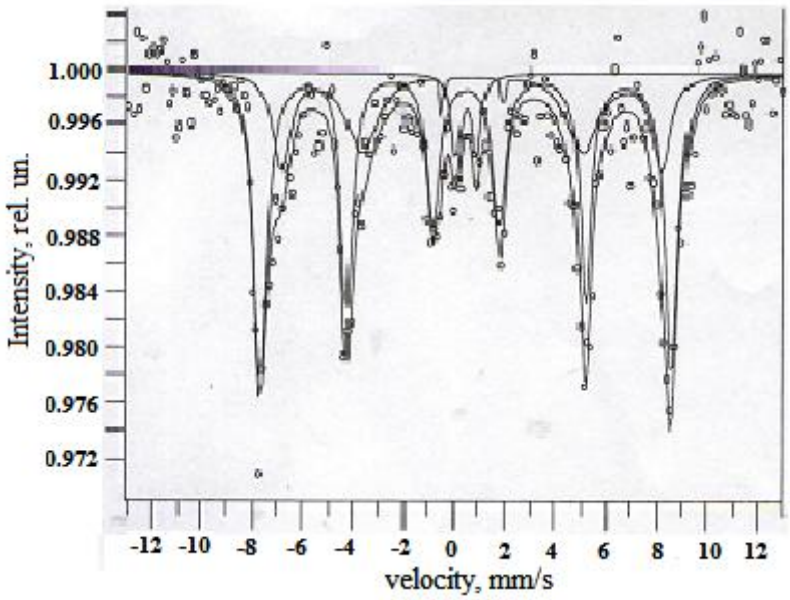

Fig. 44 The Mössbauer spectrum of maghemite nanoparticles at 78 K.

The Mössbauer parameters of our spectrum are given in Tables 14.

Table 14. The Mössbauer parameters of 14 nm maghemite nanoparticles at 78 K.

Doublet

***A* (imp.)**	***Γ*, mm/s**	***IS*, mm/s**	***QS*, mm/s**	**%**
-0.006 ± 0.002	0.429 ± 0.158	0.423 ± 0.053	0.819 ± 0.101	5.48

Sextets

***A1* (imp.)**	***A2* (imp.)**	***A3* (imp.)**	***Γ1*, mm/s**	***Γ2*, mm/s**	***Γ3*, mm/s**	***IS*, mm/s**	***QS*, mm/s**	***B*, T**	**%**
-0.022 ±0.002	-0.017 ±0.002	-0.011 ±0.002	0.656 ±0.072	0.551 ±0.081	0.625 ±0.125	0.415 ±0.014	0.032 ±0.027	50.351 ±0.119	62.72
-0.007 ±0.001	-0.006 ±0.001	-0.025 ±0.842	0.846 ±0.270	1.516 ±0.089	0.036 ±0.674	0.635 ±0.038	0.064 ±0.075	46.458 ±0.529	31.80

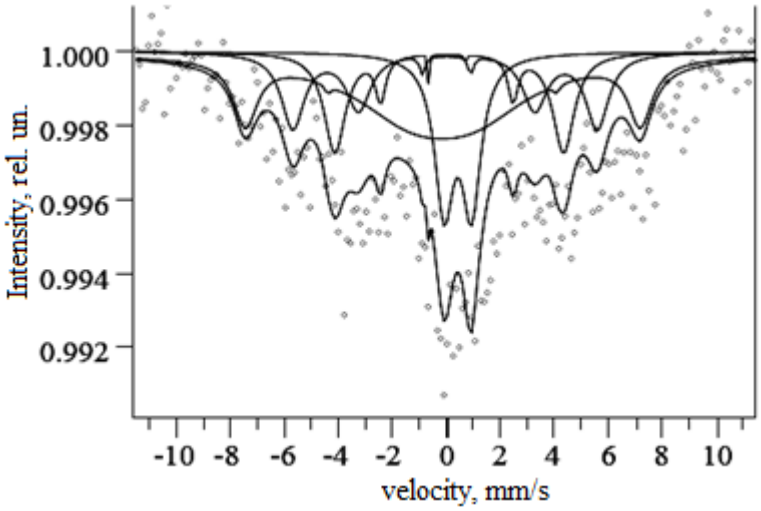

Fig. 45 The Mössbauer spectrum of 14 nm maghemite nanoparticles at 300 K.

The Mössbauer parameters of our spectrum are given in Tables 15.

Table 15. The Mössbauer parameters of 14 nm maghemite nanoparticles at 300 K.

Doublet

***A* (imp.)**	***Γ*, mm/s**	***IS*, mm/s**	***QS*, mm/s**	**%**
-0.004 ± 0.000	0.847 ± 0.153	0.375 ± 0.042	1.012 ± 0.071	17.50

Sextets

***A1* (imp.)**	***A2* (imp.)**	***A3* (imp.)**	***Γ1*, mm/s**	***Γ2*, mm/s**	***Γ3*, mm/s**	***IS*, mm/s**	***QS*, mm/s**	***B*, T**	**%**
-0.002 ±0.000	-0.000 ±0.001	-0.001 ±0.001	1.057 ±0.385	0.279 ±0.836	5.282 ±8.323	-0.191 ±0.135	-0.027 ±0.256	45.405 ±0.569	46.48
-0.002 ±0.001	-0.002 ±0.001	-0.000 ±0.001	1.019 ±0.411	1.082 ±0.639	0.227 ±0.561	-0.068 ±0.064	0.059± 0.114	35.008 ±0.511	19.47
-0.003 ±0.001	-0.001 ±0.001	-0.026 ±19.93	0.960 ±0.320	0.447 ±0.195	0.005 ±1.841	0.012 ±0.072	-0.087 ±0.122	26.312 ±0.449	16.55

For more detailed study of the structure, the spectra of the same sample are measured in an external magnetic field. As mentioned before, this sample consists of spherical maghemite particles with a diameter of 14 nm.

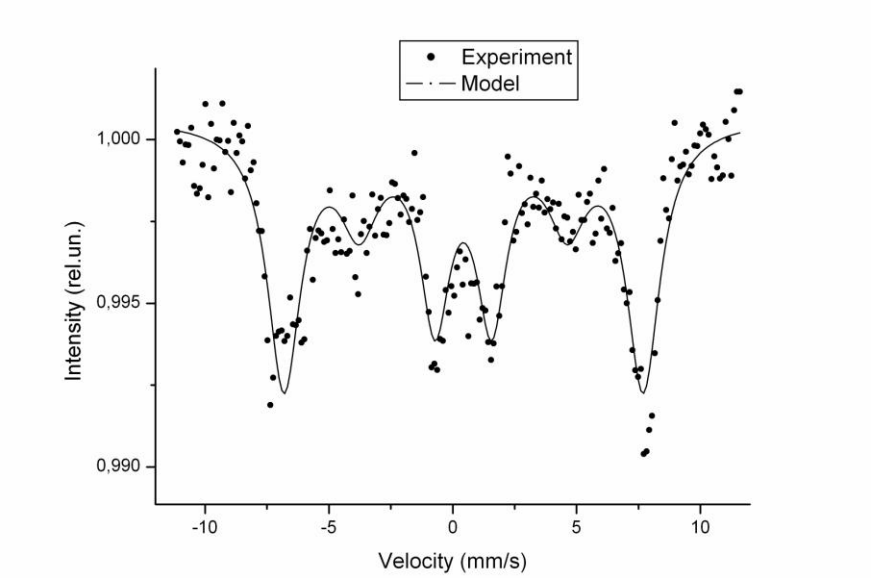

Fig. 46 The Mössbauer spectrum of 14 nm maghemite nanoparticles in an applied external magnetic field, T = 300 K.

One spectrum was measured by applied a 0.3 T magnetic field, at room temperature in the Mössbauer laboratory of Saint Petersburg State University. The direction of the external magnetic field was parallel to the direction of the gamma rays. This spectrum has one sextet of lines with an isomer shift of 0.43 mm/s and a hyperfine field of 45 T.

As is well known from the theory (see above), the intensity of our spectral lines should follow the ratio: 3:0:1:1:0:3 in a parallel external magnetic field. However, apparently from Fig. 46, total disappearance of the second and fifth spectral lines it is not observed. In our case presence of lines, which are responsible for transitions 1/2→1/2,-1/2 →-1/2, can be explained by small value of the magnetic field (0.3 T). At such a low magnetic field a part of the magnetic moments remains unordered along the external field direction.

In our experimental spectrum the calculated average θ angle is 28°.

A second spectrum of the same sample was measured in the Physics Department of Åbo Academy (see Fig. 47). The spectrum was obtained with an external magnetic field applied in a direction perpendicular to the direction of

gamma-quanta. In this case, the value of our external magnetic field was equaled 0.5 T.

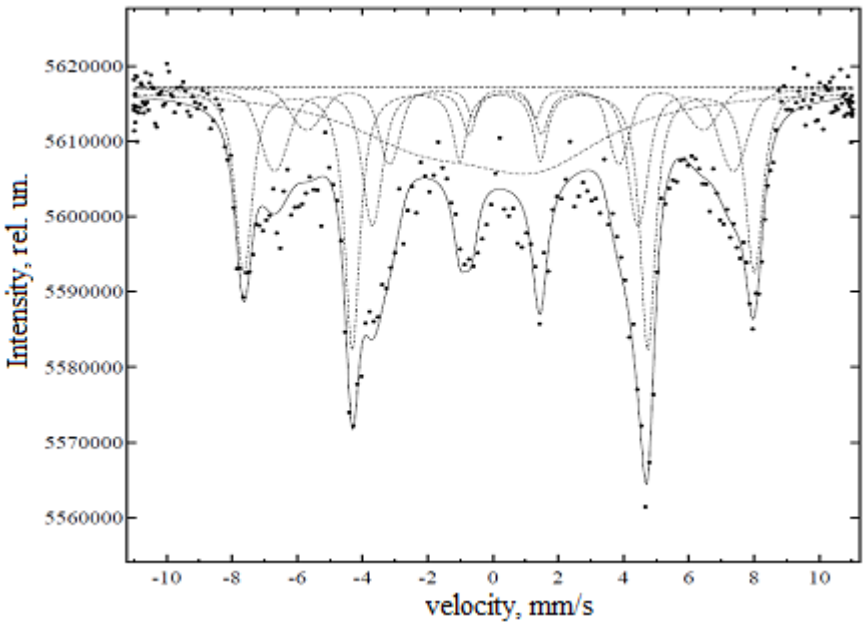

Fig. 47 The Mössbauer spectrum of 14 nm maghemite nanoparticles with an applied external magnetic field of 0.5 T.

Apparently, under such a configuration of the external field, the intensities of the second and fifth lines increase, however their parity does not quite reach the theoretical value. Again it is due to small value of the applied magnetic field as in the previous case. The calculated average angle θ between the direction of the internal magnetic field and the direction of gamma-quanta was 67° in our spectrum.

One can see from Fig. 47, with such value of the external magnetic field the structure of Mössbauer spectrum starts to resolve into components.

In the present work the Mössbauer spectra of maghemite was measured as a function of the particle size.

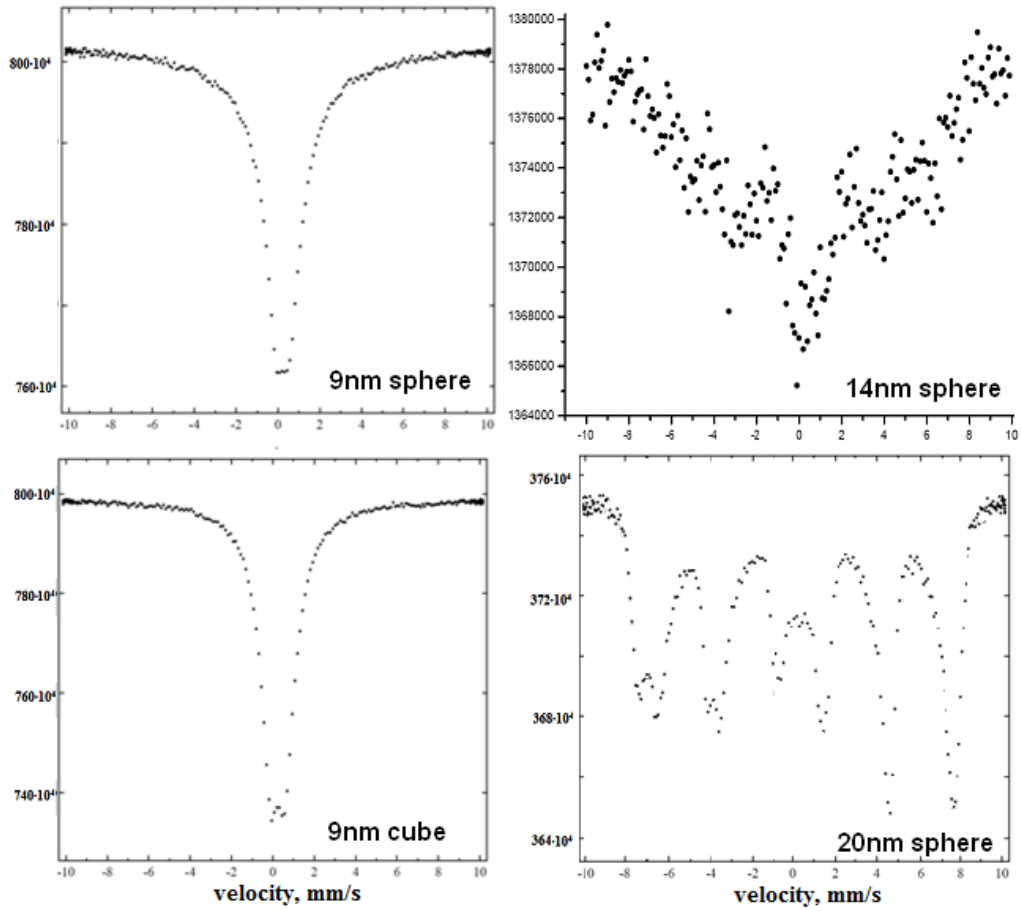

Fig. 48 The Mössbauer spectra at room temperature for samples with particle diameters of 20 nm, 14 nm and 9nm.

.

The room temperature spectra for the γ-Fe_2O_3 samples with different diameter are shown in Fig. 48. From this figure we can see that the superparamagnetic relaxation began to play a more and more appreciable role when decreasing the particle sizes. For the smaller particles, the spectrum shows only a paramagnetic doublet. Thus, the magnetic transition occurs at a lower temperature for particles with the smaller diameter.

Comparing the obtained spectra to the literature data it is possible to notice that for nanoparticles with the diameter 20 nm and more, the shape of the spectra does not differ from bulk samples. However, with further reducing the diameter, particles start to show the superparamagnetic behavior, i.e. a paramagnetic component appears in the spectrum.

Conclusions

The results of this work give following conclusions:

1. In Mössbauer spectra of nanoparticles the most typical changes in comparison with bulk phase is a broadening of the spectral lines and presence of relaxation effects. This can be connected to the decrease in the ordering temperatures and to the increase of disorder of hyperfine fields in the nanoparticles.

2. Reduction of the hyperfine field of the iron nuclei is observed for the majority of nanoparticles; the transition from bulk phase to nanoscale particles (up to sizes of 20 nm) does not lead to a decrease of the hyperfine field in comparison with bulk samples; for smaller particles (10 nm and less) the size of the hyperfine magnetic field decreases considerably in comparison with bulk values.

   The conclusions formulated in items 1 - 2 are based on the literature data and on results of our measurements.

3. Significant changes in isomer shift and quadrupole splitting values for nanoparticles, in comparison with similar bulk phases, was not observed. However, this conclusion demands more careful analysis because a considerable scattering of the quadrupole splitting and isomer shift values both for nanoparticles and bulk materials is reported.

4. Practically in all spectra of nanoparticles exist additional sextets. However these sextets are not always connected with the occurrence of other oxide phases. In certain cases it is possible to assume that the additional sextets correspond to surface atoms of nanoparticles, having, as a rule, smaller hyperfine fields in comparison with atoms in the core of the particles.

References:

[1] Suzdalev I.P., 2006. Nanotechnology: Physics and Chemistry of nanoclusters, nanostructures and nanomaterials. Moscow, KomKniga (in Russian).

[2] Goldanskiy V.I. et al. eds., 1970. Mössbauer spectroscopy: applications to chemistry. Moscow, Mir (in Russian).

[3] Semenov V.G., Moskvin L.N., Yefimov A.A., 2006. Mössbauer spectroscopy in chemical analysis. Russian Chemical Revews, 75, p. 354 (in Russian).

[4] Hanna S.S., Heberle J., et al., 1960. Phys. Rev. Letters, 4, p. 177.

[5] Shirane G., Cox D.E., Ruby S.L., 1962. Phys. Rev., 125, p. 1158.

[6] Kistner O.C., Sunyar A.W., 1960. Phys. Rev. Letters, 4, p. 412.

[7] Babanin V.F., Trukhin V.I., et al., 1995. Soil magnetism. Yaroslavl: YGU (in Russian).

[8] Bauminger R., Cohen S.G., et. al., 1961. Phys. Rev., 122, p. 1447.

[9] Verwey E.J., 1939. Nature, London, 144, p. 327.

[10] Yonezo Maeda et al., 1987. Bull. Chem. Soc. Jpn., 60, pp. 3241 - 3246.

[11] Gangopadhyay S. et al., 1992. Phys. Rev. B, 45, p. 9778.

[12] Bodker F., Morup S., and Linderoth S., 1994. Phys. Rev. Lett., 72, p. 282.

[13] Linderoth S., Morup S. and Bentzon M.D., 1995. J. Mater. Sci., 30, p. 3142.

[14] Slawska-Waniewska A., Roig A. et al., 2004. Phys. Rev. B, 70, p. 054412

[15] Topsoe H., Dumesic J.A. and Boudart M., 1974. Journal de physique, Colloque C6, supplement au n^0 12, Tome 35, page C6 - 411.

[16] Coey J.M.D. and Morrish A.H., 1971. Journal de physique, Colloque C1, supplément au n^0 2-3, Tome 32, page C1 - 271.

[17] Morrish A.H. and Haneda K., 1980. Journal de physique, Colloque C1, supplément au n^0 1, Tome 41, page C1 - 171.

[18] Morrish A.H., Haneda K. and Schurer P.J., 1976. J. Physique Colloq., 37, p. C6 - 301.

[19] Haneda K.and Morrish A.H., 1977. Solid State Commun, 22, p. 779.

[20] Haneda K. and Morrish A.H., 1978. Surf. Sci., 77, p. 584.

[21] Nikolaev V.I., Shipilin A.M., Zakharova I.N., 2001. Journal of Solid-State Physics, Vol.43, issue 8, p. 1455 (in Russian).

[22] Saeed Kamali-M, Tore Ericsson, Roger Wäppling, 2006. Thin Solid Films, 515, pp. 721 - 723.

[23] Lennart Häggström et al., 2008. Hyperfine Interactions, 183, 1 - 3, pp. 221 - 225.

[24] Salazar-Alvarez G. et al., 2008. J. Am. Chem. Soc., 130, pp. 13234 - 13239.

[25] Kundu T.K. et al., 1988. Journal of Materials Science, 33, pp. 1759 - 1763.

[26] Sinha T.P. et al., 1996. Ind. J. Phys., 70A, p. 741.

[27] Suzdalev I.P. et al., 2001. Russian Chemical Journal, Vol. XLV, 3, p. 66 (in Russian).

[28] Suzdalev I.P. et al., 2006. Nanotechnologies in Russia, Vol. 1, 1 - 2, p. 134 (in Russian),

[29] Gorozhankin D.F. et al., 2004. Doklady Chemistry, Vol. 396, Part 2, pp. 132 - 135.

[30] Anwar Ahniyaz et al., 2008. J. of Magn. Magn. Mater., 320, pp. 781 - 787.

[31] Mashukov A.V., Mashukova A.E., Siminchuk S.A., State University of non-ferrous metals and gold, Russia, "Hyperfine interaction in iron-containing minerals" (in Russian),
http://www.rusnauka.com/NIO/Phisica/mashukov%20a.v..doc.htm

[32] Armstrong R.J., Morrish A.H., and Sawatzky G.A., 1966. Phys. Lett., 23, p. 414.

[33] Kündig W. and Hargrove R.S., 1969. Solid State Commun., 7, p. 223.

[34] Bowen L.H., De Grave E. and Bryan A.M., 1994. Hyperfine Interactions, 94, p. 1977.

[35] Suzdalev I.P. et al., 2006. Nanotechnologies in Russia, Vol. 1, 1 - 2, pp. 46- 57 (in Russian).

[36] Vasilyeva E.S et al., 2007. JETF Letters, Vol. 33, issue 1, pp. 81 – 87 (in Russian),

[37] Kündig W. and Bömmel H., 1966. Phys. Rev., 142, p. 327.

[38] Bayburtskiy F. S., Senatskaya I. I., Baldokhin Yu. V., Solomatin A. S. (in Russian),
http://magneticliquid.narod.ru/autority/009.htm.

[39] Edelman I.S. et al., 2008. Journal of Solid-State Physics, Vol. 50, issue 12, pp. 2192 - 2197 (in Russian).

Appendix 1

Table of Mössbauer parameters of bulk samples of iron oxide.

Sample	***QS*, mm/s**	***IS*, mm/s**	***B*, T**	**Ref., #**	***T*, K**
α-Fe_2O_3	-0.21	0.74*	51.8	**[7]**	298
	0.34		54.2		78
			54.5		4
α-Fe_2O_3	0.24 ± 0.03	0.47 ± 0.03**	51.5	**[2]**	300
α-Fe_2O_3	-	0.314	-		295
γ-Fe_2O_3	0,02	0.37*	49.9	**[7]**	298
		0.46*	52.7		78
γ-Fe_2O_3	-0.1 ± 0.1	0.5 ± 0.05**	50.5	**[2]**	300
	0.1 ± 0.1	0.4 ± 0.1**	51.5		78
γ-Fe_2O_3			49.4	**[32]**	298
γ-Fe_2O_3			52.6	**[34]**	4.2
Fe_3O_4	0.005	0.059*	50.7	**[7]**	300
	0.003	0.086*	45.0		
Fe_3O_4			51.5	**[7]**	77
Fe_3O_4	-	-	48.5	**[31]**	300
	-	-	47.2		
Fe_3O_4			49.2	**[33]**	300
			46.1		
$Fe_{0.941}O$	0.30	1.15		**[5]**	300
$Fe_{0.919}O$	0.34	1.15			
$Fe_{0.915}O$	0.32	1.15			

* Isomer shift is measured relative to sodium nitroprussid.

** Isomer shift is measured relative to stainless steel.

Appendix 2

Summary table of the Mössbauer parameters of iron oxide nanoparticles.

Sample	***Γ₁*** **mm/s**	***QS*****, mm/s**	***IS*****, mm/s**	***B*****, T**	**#**	***T*****, K**	**Size of particles**
γ-Fe_2O_3	0.55	0.00 (± 0.01)	0.442 (± 0.005)	48.7	**[23]**	5	spherical *d* = 4 nm
γ-Fe_2O_3	0.49	0.00 (± 0.01)	0.440 (± 0.005)	51.3	**[23]**	5	spherical *d* = 12 nm
γ-Fe_2O_3	0.58	0.00 (± 0.01)	0.443 (± 0.005)	51.3	**[23]**	5	cube *l* = 9 nm
γ-Fe_2O_3		0.00	0.451	49.8	**[10]**	4.2	
γ-Fe_2O_3	0.62	0	0.50 ± 0.03	47.8	**[28]**	4.2	2 – 3 nm
γ-Fe_2O_3	0.55	0.00	0.442	48.7	**[23]**	5	*d* = 4 nm spherical
	0.49	0.00	0.440	51.3			*d* = 12 nm spherical
	0.58	0.00	0.443	51.3			cube *l* = 9 nm
γ-Fe_2O_3			0.442	48.4	**[30]**	5	*d* = 4 nm spherical
γ-Fe_2O_3	0.657	-0.275	0.549	49.2	**[10]**	78	Needle-shaped, *d* = 15 nm, *l* = 100 nm, *d*(Me) = 12.2 nm
γ-Fe_2O_3	1.398	-0.336	0.585	48.7	**[10]**	78	Needle-shaped, *d* = 15 nm, *l* = 100 nm, *d*(Me) = 10.6 nm
γ-Fe_2O_3	1.199	-0.245	0.575	49.0	**[10]**	78	Needle-shaped, *d* = 15 nm, *l* = 100 nm, *d*(Me) = 9.8 nm
γ-Fe_2O_3	1.208	-0.280	0.562	48.9	**[10]**	78	Needle-shaped, *d* = 15 nm, *l* = 100 nm, *d*(Me) = 9.2 nm
γ-Fe_2O_3	1.231	-0.009	0.487	48.8	**[10]**	78	Needle-shaped, *d* = 15 nm, *l* = 100 nm, *d*(Me) = 8.4 nm

γ-Fe_2O_3	1.315	+0.079	0.463	48.8	**[10]**	78	Needle-shaped, d = 15 nm, l = 100 nm, d(Me) = 8.8 nm
γ-Fe_2O_3		0.00			**[35]**	77	20 – 50 nm
γ-Fe_2O_3		0.87 ± 0.03	0.47 ± 0.03		**[29]**	78	2 – 3 nm
γ-Fe_2O_3		0.00 ± 0.02		47.0	**[29]**	78	30 – 50 nm
γ-Fe_2O_3			0.31		**[30]**	295	4 nm
γ-Fe_2O_3		0.10	0.40	50.5	**[38]**	300	12 nm
γ-Fe_2O_3	0.26 ± 0.03	0.43 ± 0.03	0.33 ± 0.02	50.1	**[39]**	300	30 – 70 nm
Fe	0.405		0.168	34.5	**[10]**	78	Needle-shaped, d = 15 nm, l = 100 nm, d(Me) = 12.2 nm
Fe	0.388		0.170	34.5	**[10]**	78	Needle-shaped, d = 15 nm, l = 100 nm, d(Me) = 10.6 nm
Fe	0.440		0.163	34.5	**[10]**	78	Needle-shaped, d = 15 nm, l = 100 nm, d(Me) = 9.8 nm
Fe	0.412		0.163	34.5	**[10]**	78	Needle-shaped, d = 15 nm, l = 100 nm, d(Me) = 9.2 nm
Fe	0.469		0.171	34.6	**[10]**	78	Needle-shaped, d = 15 nm, l = 100 nm, d(Me) = 8.4 nm
Fe	0.542		0.170	34.6	**[10]**	78	Needle-shaped, d = 15 nm, l = 100 nm, d(Me) = 8.8 nm
Fe			0.12	34.2	**[13]**	5	d = 2 nm
Fe				30.2	**[13]**	5	d = 2 nm, 4,3 T ↑↓ γ
α -Fe_2O_3		-0.29			**[35]**	77	20 – 50 nm
α -Fe_2O_3		-0.29 ± 0.02		52.0	**[28]**	78	30 – 50 nm
α -Fe_2O_3				52.7	**[37]**	78	18 nm
α -Fe_2O_3		0.78	0.42		**[35]**	120	20 – 50 nm
α-Fe_2O_3		0.24	0.47	51.7	**[38]**	300	12 nm

α-Fe_2O_3	0.27 ± 0.03	-0.32 ± 0.03	0.38 ± 0.02	51.6	**[39]**	300	30 – 70 nm
Fe_3O_4				47.0	**[36]**	300	12 nm
Fe_3O_4			0.43*	49.0	**[16]**	300	Fe^{3+}(A)
			0.83*	46.3			$Fe^{3+/2+}$(B)
Fe_3O_4			0.51		**[37]**	295	4 nm
Fe_3O_4		0.1	0.45	49.0	**[38]**	300	12 nm
		0.0	0.7	45.0 - 46.0			
Fe_3O_4				40.7	**[21]**	295	Fe^{2+},Fe^{3+} (A,B site) on surface, 7.5 nm
				43.1			
				45.6			Fe^{2+},Fe^{3+} (A,B site) inside of particle, 7.5 nm
				48.2			
Fe_3O_4				49.6	**[14]**	80	d = 15 nm

* Isomer shift is measured relative to chromium.